Title: Neuropeptide Y regulates sleep by modulating noradrenergic signaling

Authors: Chanpreet Singh[1], Jason Rihel[2] and David A. Prober[1*]

Affiliations: [1]Division of Biology and Biological Engineering, California Institute of Technology, Pasadena, CA, 91125, USA; [2]Department of Cell and Developmental Biology, University College London, London, WC1E 6BT, UK.

[*]**Corresponding author:** dprober@caltech.edu

Lead Contact: David A. Prober

SUMMARY

Sleep is an essential and evolutionarily conserved behavioral state whose regulation remains poorly understood. To identify genes that regulate vertebrate sleep, we recently performed a genetic screen in zebrafish, and here we report the identification of neuropeptide Y (NPY) as both necessary for normal daytime sleep levels and sufficient to promote sleep. We show that overexpression of NPY increases sleep, whereas mutation of *npy* or ablation of *npy*-expressing neurons decreases sleep. By analyzing sleep architecture, we show that NPY regulates sleep levels primarily by modulating the length of wake bouts. To determine how NPY regulates sleep, we tested for interactions with several systems known to regulate sleep, and provide anatomical, molecular, genetic and pharmacological evidence that NPY promotes sleep by inhibiting noradrenergic signaling. These data establish NPY as an important vertebrate sleep/wake regulator and link NPY signaling to an established arousal-promoting system.

Key words: Sleep, neuropeptide Y, hypothalamus, locus coeruleus, noradrenaline, locomotor activity, arousal, genetics

HIGHLIGHTS:

- A genetic screen in zebrafish shows that overexpression of NPY promotes sleep
- Mutation of *npy* or ablation of *npy*-expressing neurons results in decreased sleep
- NPY regulates sleep levels primarily by modulating the length of wake bouts
- NPY promotes sleep by inhibiting noradrenergic signaling

eTOC Blurb

Based on a genetic screen, Singh et al identify NPY signaling and *npy*-expressing neurons as regulators of zebrafish sleep. They show that NPY promotes sleep by inhibiting noradrenergic signaling, thus linking NPY signaling to an established arousal-promoting system.

INTRODUCTION

Sleep is among most basic needs of living organisms, yet mechanisms that regulate sleep remain poorly understood. Several neuropeptides have been implicated in regulating mammalian sleep [1], including hypocretin [2-4], which promotes wakefulness, and galanin [5-8] and melanin concentrating hormone [9-12], which promote sleep, suggesting that examining additional neuropeptides may be a fruitful approach to identify novel mechanisms that regulate sleep. Identifying these mechanisms using mammalian model systems has been challenging due to their poor amenability for large-scale screens, although such screens are possible [13]. As an alternative approach, several groups have used behavioral criteria to study sleep-like states in simpler model organisms that are amenable to screens, including *Drosophila* [14, 15], *C. elegans* [16, 17], and zebrafish [18-20]. In particular, several groups have demonstrated behavioral, anatomical, genetic and pharmacological conservation of sleep between zebrafish and mammals, establishing zebrafish as a simple and inexpensive vertebrate sleep model [18-24]. We previously described a novel approach that we used to screen for genes whose overexpression affects zebrafish sleep, and reported that the neuropeptide neuromedin U is both necessary and sufficient for normal levels of arousal [25]. Here we demonstrate that another neuropeptide identified in the screen, neuropeptide Y (NPY), is both necessary for daytime sleep and sufficient to promote sleep.

NPY is widely expressed in the brain and has been implicated in regulating several endocrine, behavioral and circadian processes in mammals (reviewed in [26]). NPY is perhaps best known for its role in promoting feeding [27-30]. NPY has also been shown to affect sleep, but its role in this behavioral state remains unclear. Several studies showed that injection of *in vitro* synthesized NPY into the rodent brain [31-37] or intravenously in young healthy [38] or depressed [39] human subjects can induce sleep or reduce locomotor activity. However, other rodent studies reported the opposite effect [40-42]. The basis for these disparate reports is unclear, but may be due to

different sites and doses of NPY injection, or the use of *in vitro* synthesized peptide that may vary in different preparations and from endogenously produced NPY. Understanding the role of NPY in mammalian sleep is also confounded by extensive links between mechanisms that regulate feeding and sleep [40-43]. Indeed, the wake-promoting effect of injected NPY is associated with increased feeding [40-42], suggesting that the increase in wakefulness may be an indirect effect of NPY on feeding. *npy* mutant mice exhibit several phenotypes, including increased anxiety in the open field test, depression-like behavior in the forced swim test, and cognitive deficits in the Morris water maze [44, 45], and are less susceptible to diet-induced obesity as a result of reduced feeding and increased energy expenditure [46]. However, an analysis of sleep in these animals and a role for *npy*-expressing neurons in sleep has not been described. As a result, despite decades of study, the role of NPY in vertebrate sleep remains unclear.

Here we use a genetic screen and follow-up gain-of-function genetic studies to show that NPY is sufficient to promote sleep in zebrafish. Using an *npy* mutant and chemogenetic ablation of *npy*-expressing neurons, we also show that endogenous *npy* and *npy*-expressing neurons are necessary for normal daytime sleep levels. Finally, we show that NPY promotes sleep by inhibiting the wake-promoting noradrenergic system, thus providing a mechanistic basis for the regulation of sleep by NPY. Taken together with the requirement of noradrenergic signaling for the wake-promoting function of hypocretin [47, 48], these results suggest that the noradrenergic system integrates neuropeptidergic signals that regulate sleep/wake states.

RESULTS

Overexpression of human NPY reduces locomotor activity and increases sleep in zebrafish larvae

We recently performed a genetic overexpression screen to identify genes that affect larval zebrafish sleep and wakefulness [25]. In the primary screen, we injected over 1200 unique

plasmids in which a heat shock-inducible promoter (*hsp*) regulates the expression of genes that encode for secreted proteins into wild-type (WT) zebrafish embryos at the one-cell stage. We used a collection of human open reading frames (ORFs) encoding secreted proteins from the hORFeome 3.1 library [49] because a resource of zebrafish ORFs was not available. Co-injection of each plasmid with *tol2 transposase* mRNA resulted in efficient incorporation of the *hsp* regulated transgene into the genome in many cells of each animal and enabled heat shock-induced overexpression [25]. We then compared sleep/wake behaviors in injected animals before and after heat shock and to negative control animals injected with a *hsp:egfp* plasmid. One gene whose overexpression increased sleep at night (Z-score=1.8) encoded human NPY (**Figure S1A**). Even though zebrafish larvae normally exhibit high levels of sleep at night, we found that overexpression of human NPY caused a further 28% decrease in locomotor activity and 34% increase in sleep compared to control animals during the night following heat shock ($P<0.05$ and $P<0.01$, two-tailed Student's *t* test) (**Figures S1B-S1G**). We observed a similar phenotype during the day before heat shock that did not reach statistical significance, consistent with leaky expression from the *hsp* promoter that often is observed using this transient injection assay, but is not observed using stable transgenic lines [25].

Overexpression of zebrafish NPY reduces locomotor activity and increases sleep in zebrafish larvae

Based on the human NPY overexpression phenotype, we investigated the role of the zebrafish *npy* orthologue in sleep. Using reciprocal BLAST searches, we identified a single *npy* ortholog in the zebrafish genome, which encodes for a preproprotein that generates a predicted 36 amino-acid mature peptide that is 89% identical to the mature peptide of human and mouse NPY (**Figure S1H**). *npy* is widely expressed in the mammalian brain, particularly in the hypothalamus, amygdala, locus coeruleus (LC) and cerebral cortex [50, 51]. Using *in situ* hybridization (ISH) with an *npy*-specific probe, immunostaining for total extracellular signal-regulated kinase (t-ERK), and

registration of images to the Z-brain atlas [52], we found that *npy* is similarly expressed in several discrete nuclei within the larval zebrafish brain. These include the olfactory bulb, telencephalon, preoptic area, posterior tuberculum, intermediate lateral hypothalamus, caudal medial hypothalamus, pretectum, torus semicircularis, tectum, LC, medial rhombomere and subpallium (**Figures S1I–S1N and Video S1**). We also observed *npy* expression in the retina (data not shown) but not in other tissues.

To test whether overexpression of zebrafish NPY affects sleep in zebrafish, we generated *Tg(hsp:npy)* stable transgenic zebrafish. We observed that *Tg*(*hsp*:*npy*) animals and their WT siblings exhibited similar levels of locomotor activity and sleep before heat-shock (**Figures 1A-1D**)**.** However, following a heat shock at 3 p.m., *Tg(hsp:npy)* animals were 50% less active (**Figures 1A and 1B**) and slept 111% more (**Figures 1C and 1D**) than their WT siblings for the rest of the day (both $P<0.0001$, two-tailed Student's *t* test). The phenotype resulted from a 230% increase in the number of sleep bouts (**Figure 1E**) and an 85% decrease in the length of wake bouts (**Figure 1G**) (both $P<0.0001$, two-tailed Student's *t* test), with a smaller decrease in the length of sleep bouts (**Figure 1F**), and thus is primarily due to fragmentation of the wake state.

The increase in sleep after the heat shock-induced pulse of NPY overexpression was dampened by nighttime. A previous study showed that the circadian system inhibits sleep in the evening, when homeostatic sleep drive is high [53], suggesting the circadian system might limit NPY overexpression-induced sleep to the day. To test whether NPY overexpression can also increase sleep at night, we heat shocked animals during the last hour of the day. We found that *Tg(hsp:npy)* animals were 46% less active (**Figures S2A-S2C**) and slept 54% more (**Figures S2D-S2F**) than their WT siblings during the night (both $P<0.0001$, two-tailed Student's *t* test), similar to the daytime phenotype when NPY overexpression was induced in the afternoon. The nighttime phenotype was due to an increase in the length of sleep bouts (**Figure S2H**) and a decrease in

the length of wake bouts (**Figure S2J**). Unlike NPY overexpression induced during the afternoon, there was no change in the number of sleep bouts (**Figure S2G**). These observations suggest that dampening of the NPY overexpression phenotype at night following heat shock in the afternoon is due to declining levels of overexpressed NPY rather than effects of the circadian clock on NPY function.

Light affects locomotor activity and sleep in zebrafish [19, 20], as it does in mammals [54]. To determine whether light affects NPY overexpression-induced sleep, we entrained larvae by raising them in 14:10 hour light:dark (LD) conditions for four days, and then transferred them to constant dark before inducing NPY overexpression. Overexpression of NPY decreased locomotor activity by 54% (**Figures S2K and S2L**) and increased sleep by 80% (**Figures S2M and S2N**) during the rest of the subjective day compared to WT siblings (both $P<0.0001$, two-tailed Student's *t* test). This phenotype was due to an increase in the number of sleep bouts (**Figure S2O**) and a decrease in the length of wake bouts (**Figure S2Q**), with no change in the length of sleep bouts (**Figure S2P**). Hence, NPY overexpression promotes sleep independent of lighting condition and circadian phase.

Overexpression of zebrafish NPY increases arousal threshold in zebrafish larvae

Sleep is distinguished from quiet wakefulness by reduced responsiveness to stimuli [55]. Because NPY overexpression increases sleep, we asked whether it also alters arousal threshold. To do so, we delivered mechano-acoustic tapping stimuli of variable intensities every minute to larvae after overexpression of NPY and monitored their behavioral responses. We found that the effective tap intensity at which we observed the half-maximal response (effective tap power 50, ETP_{50}) for *Tg(hsp:npy)* was 290% higher than their WT siblings (**Figure 1H**) ($P<0.05$ by extra sum-of-squares F test). Thus, NPY overexpression increases arousal threshold, consistent with a sleep state. We next asked if overexpression of NPY affects arousal in awake and/or sleeping

larvae. To do so, we delivered tapping stimuli at three tap powers of 2.3, 3.0 and 4.0 arbitrary units, which were lower than the ETP_{50} of both *Tg(hsp:npy)* and WT siblings. We allowed 5 minutes between trials and, according to the behavioral definition of sleep, scored animals as awake if they moved during the minute before a tap stimulus. We found that NPY overexpressing animals were significantly less responsive to these stimuli compared to their WT siblings during both awake (**Figure 1I**) (all intensities $P<0.0001$, two-tailed Student's *t* test), and sleep (**Figure 1J**) ($P<0.05$, $P<0.01$ and $P<0.001$ for 2.3, 3.0 and 4.0 tap powers, respectively, two-tailed Student's *t* test) states. These data suggest that NPY overexpression decreases arousal in awake animals and increases sleep depth in sleeping animals.

npy mutant zebrafish are more active and sleep less during the day

Having shown that overexpression of NPY is sufficient to promote sleep, we next asked whether endogenous *npy* is required for normal sleep/wake behaviors. To do so, we used the zinc finger nuclease method to generate zebrafish containing a predicted null mutation in the *npy* open reading frame [56]. We isolated a zebrafish line containing a 17-nucleotide deletion in the second exon of the *npy* gene [56], which results in a translational frame shift at the beginning of the mature peptide domain (**Figure 2A**), generating a protein that lacks the mature peptide domain and thus is likely nonfunctional. These homozygous mutant animals are viable and fertile, and lack obvious developmental defects.

Consistent with the NPY overexpression phenotype, *npy*-/- larvae were 23% more active and slept 36% less during the day than their *npy*+/+ siblings ($P<0.0001$ and $P<0.01$, one-way ANOVA, Holm-Sidak test) (**Figures 2B, 2C, 2E and 2F**). These effects were due to a decrease in the number of sleep bouts (**Figure 2H**) and an increase in the length of wake bouts (**Figure 2L**), with no effect on the length of sleep bouts (**Figures 2J**). Thus, reduced daytime sleep in *npy*-/- animals is due to consolidation of the wake state. We did not observe sleep/wake phenotypes in *npy*-/-

194 animals at night. These data indicate that endogenous *npy* is required for normal daytime sleep
195 levels.
196
197 Previous studies showed that microinjection of NPY into the suprachiasmatic nucleus (SCN) of
198 the hamster hypothalamus phase shifts the locomotor activity circadian rhythm in constant light
199 (LL) [57, 58], suggesting that NPY may regulate entrainment or expression of circadian rhythms.
200 To test whether endogenous *npy* is required for circadian regulation of locomotor activity and
201 sleep, we tested larvae that were entrained for 4 days in LD, then monitored for 24 hours in LD
202 and then for 48 hours after a shift to LL. Absence of *npy* had no obvious effect on the locomotor
203 activity or sleep circadian period length or phase (**Figures 3A and 3D**). As expected, in LD *npy*-
204 /- animals were more active (**Figures 3A and S3A**) and slept less (**Figures 3D and S3C**) than
205 their *npy*+/+ and *npy*+/- siblings during the day, with no phenotype at night. The daytime
206 phenotype was due to fewer sleep bouts and longer wake bouts (**Figures S3E and S3I**). Following
207 the shift to LL, *npy*-/- animals were more active by 30% and 26% during the subjective day and
208 night, respectively, compared to their *npy*+/+ siblings ($P<0.001$ and $P<0.01$, one-way ANOVA,
209 Holm-Sidak test) (**Figures 3A-3C**). *npy*-/- larvae also slept ~40% less during the subjective day
210 and night ($P<0.0001$ and $P<0.001$, one-way ANOVA, Holm-Sidak test) (**Figures 3D-3F**). These
211 phenotypes were primarily due to longer wake bouts (**Figures 3K and 3L**), although there were
212 also fewer (**Figures 3G and 3H**) and shorter (**Figures 3I and 3J**) sleep bouts. These results
213 indicate that *npy* is not required for circadian regulation of locomotor activity or sleep in zebrafish
214 larvae, but rather regulates sleep in a light-dependent manner.
215
216 **Ablation of *npy*-expressing neurons increases locomotor activity and decreases sleep**
217 As an alternative approach to test the hypothesis that NPY is necessary for normal sleep levels,
218 we used a chemogenetic approach to specifically ablate *npy*-expressing neurons. To this end, we
219 used BAC recombineering [59] to insert an optimized version of the transcriptional activator Gal4

(KalTA4) at the *npy* start codon of a BAC containing 290 kb of genomic sequence that includes the *npy* gene. We then used Tol2-mediated transgenesis to generate *Tg(npy:kalta4)* zebrafish. To determine the specificity of this transgenic line, we performed double fluorescent ISH (FISH) using probes specific for *npy* and *kalta4*. We observed that, depending on the brain region, *kalta4* is expressed in >80% of *npy*-expressing neurons (>95% for some nuclei), and that >92% of *kalta4*-expressing neurons also express *npy* (**Figure S5A and Table S1**). To ablate these neurons, we mated these fish to *Tg(uas:nfsb-mcherry)* animals [60], resulting in the expression of nitroreductase (nfsb) in *npy*-expressing neurons (**Figure 4A**). Nitroreductase is a bacterial protein that converts the inert prodrug metronidazole (MTZ) into a cytotoxic DNA crosslinking agent, thus enabling drug-inducible ablation of the targeted cell type [61]. *Tg(npy:kalta4); Tg(uas:nfsb-mcherry)* and *Tg(npy:kalta4)* sibling controls were treated with MTZ or DMSO vehicle control for 48 hours (from 3 days post-fertilization (dpf) to 5 dpf), which resulted in an almost complete elimination of mCherry-labeled cells in double transgenic animals treated with MTZ compared to DMSO (**Figures 4A-4C**), indicating the loss of most *npy*-expressing neurons. Consistent with these observations, we detected extensive TUNEL labeling in *npy*-expressing neurons in *Tg(npy:kalta4);Tg(uas:nfsb-mcherry)* larvae treated with MTZ, but not in those treated with DMSO (**Figures S5B-S5D**)**,** indicating that MTZ treatment induces apoptosis of *npy*-expressing neurons. Consistent with the *npy*-/- phenotype, we found that ablation of *npy*-expressing neurons caused a 23% increase in locomotor activity (**Figures 4C and 4D**) and a 28% decrease in sleep (**Figures 4F and 4G**) ($P<0.01$ and $P<0.05$, two-tailed Student's *t* test) compared to sibling controls during the day. This phenotype was due to a decrease in the number of sleep bouts (**Figure 4I**) and an increase in the length of wake bouts (**Figure 4M**), indicating consolidation of the wake state, similar to *npy*-/- animals. To confirm that the *Tg(uas:nfsb-mcherry)* transgene does not induce a behavioral phenotype in the absence of *Tg(npy:kalta4)*, we crossed *Tg(npy:kalta4)/+;Tg(uas:nfsb-mcherry)/+* to WT fish, excluded animals that were positive for mCherry, and treated the remaining animals with MTZ. We observed no difference in

locomotor activity or sleep levels among animals of these three genotypes (**Figure S4**). The cell ablation phenotype was slightly weaker than that of the *npy* mutant, likely because the *npy:kalta4* transgene is not expressed in all *npy*-expressing neurons. A caveat to this experiment is that a small number of neurons express *kalta4* but not *npy* in some brain regions (8% of KalTA4-positive cells in the subpallium, <5% of KalTA4-positive cells in other brain regions; **Figure S5A and Table S1**). As a result, it is possible that ablation of these NPY-negative cells is responsible for the behavioral phenotype. However, this is unlikely to be the case due to the small number of cells involved and because the NPY neuron ablation phenotype is consistent with the *npy* mutant phenotype, suggesting that both NPY and *npy*-expressing neurons are necessary for normal daytime sleep levels.

The NPY overexpression phenotype is not blocked by manipulation of several pathways known to regulate sleep

To identify genetic mechanisms through which NPY affects sleep, we tested whether the NPY overexpression phenotype is suppressed in zebrafish containing mutations in other genes implicated in regulating sleep (**Table S2**). We found that the NPY overexpression phenotype persisted in larvae containing null mutations in *histidine decarboxylase* (*hdc*) [62], *hypocretin receptor* (*hcrtr*) [19], *corticotropin releasing hormone a* (*crha)* (Singh et al., unpublished)*, crhb* (Singh et al., unpublished) or arylalkylamine *N-acetyltransferase 2* (*aanat2*) [63] (data not shown). These data suggest that NPY promotes sleep via other mechanisms.

NPY promotes sleep by inhibiting noradrenergic signaling

Pharmacological and genetic studies in mammals and zebrafish have shown that norepinephrine (NE) plays an important role in promoting arousal [48, 64], and the brainstem LC is the primary source of NE in the brain [65]. We obtained several lines of evidence suggesting that NPY promotes sleep by inhibiting NE signaling. First, a nucleus of 3-5 *npy*-expressing neurons is

located adjacent to, and sends projections that form close contacts with, LC neurons (**Figures 5A-5H and Video S2**). While this observation does not prove a direct interaction between the two neuronal populations, it is consistent with our functional evidence that NPY promotes sleep by inhibiting NE signaling (see below). The zebrafish genome contains at least seven *npy receptor* genes [66]. To determine if one or more of these receptors is expressed in LC neurons, we performed FISH using probes specific for each receptor in *Tg(dbh:EGFP)* larvae [67], whose LC neurons express EGFP. We did not detect expression of any *npy receptor* in LC neurons, although we observed expression of *npy receptor y1* (*npyr1*) (**Figure 5I**) and *npy receptor y2 like* (*npyr2l*) (**Figure 5J**) in cells near the LC. The other *npy receptors* either showed specific expression in other brain regions (*npyr8a* and *npyr8b*) or no detectable specific pattern of expression (*npyr2*, *npyr4* and *npyr7*) (data not shown). These results suggest that NPY may indirectly affect NE signaling, although it remains possible that a *npy receptor* is expressed in LC neurons at levels too low to be detected using FISH, a common problem for G-protein coupled receptors (GPCRs), the protein class of NPY receptors.

Second, we found that the sedating effects of NPY overexpression and loss of NE signaling are not additive. We made this observation by overexpressing NPY in larvae that lack NE synthesis due to mutation of *dopamine beta hydroxylase* (*dbh*) [48], or that lack NE signaling due to treatment with the α-1-adrenergic receptor antagonist prazosin. Both genetic and pharmacological inhibition of NE signaling increase sleep in zebrafish larvae [48]. If NPY promotes sleep by inhibiting NE signaling, then overexpression of NPY should not further increase sleep in *dbh*-/- larvae or in WT larvae treated with prazosin. Alternatively, if NPY promotes sleep via a NE-independent mechanism, then the combined effects of NPY overexpression and loss of NE signaling on sleep should be additive. Because the behavior of *dbh*+/- animals is indistinguishable from that of their *dbh*+/+ siblings [48], we compared *dbh*+/- and *dbh*-/- siblings to reduce the number of comparisons in each experiment, and thus increase the number of

298 animals per condition. Prior to heat shock-induced NPY overexpression, *dbh*-/- larvae were 40%
299 less active and slept over 100% more than their *dbh*+/- siblings for both *Tg(hsp:npy)* larvae and
300 their non-transgenic siblings (**Figures 6A-6D**) (both: $P<0.01$, two-way ANOVA, Holm-Sidak test).
301 Overexpression of NPY decreased locomotor activity by 54% and increased sleep by 60% in
302 *Tg(hsp:npy);dbh*+/- larvae compared their *dbh*+/- siblings (**Figures 6A-6D**) ($P<0.0001$ and
303 $P<0.05$, Two-way ANOVA, Holm-Sidak test). However, overexpression of NPY did not further
304 affect the sleep/wake behavior of *dbh-/-* larvae, as locomotor activity and sleep levels were
305 indistinguishable for *Tg(hsp:npy);dbh-/-* and *dbh-/-* larvae (**Figures 6A-6D**). We obtained similar
306 results for NPY overexpression in prazosin-treated larvae to compared to DMSO vehicle-treated
307 controls (**Figures S6A-S6D**). To confirm that the failure of NPY overexpression to enhance sleep
308 in *dbh*-/- or prazosin-treated animals is not due to a ceiling effect for sleep, we found that treatment
309 with melatonin, an alternative sedative, enhanced sleep induced by overexpression of NPY
310 (**Figures S7A-S7D**) or prazosin (**Figures S7E-S7H**).
311
312 Third, we found that the increased locomotor activity and reduced sleep observed in *npy*-/-
313 animals compared to their *npy*+/+ siblings was abolished by treatment with prazosin. We made
314 this observation by treating *npy*+/+, *npy*+/- and *npy*-/- larvae with either DMSO or prazosin. If NPY
315 promotes sleep by inhibiting NE signaling, then loss of NPY should not affect prasozin-induced
316 sleep. Alternatively, if NPY promotes sleep via a NE-independent mechanism, then loss of NPY
317 should affect sleep amount in prazosin-treated animals. Consistent with the former possibility, we
318 found that prazosin decreased locomotor activity and increased sleep, and this phenotype was
319 indistinguishable for *npy*+/+, *npy*+/- and *npy*-/- siblings (**Figures 6E-6J**).
320
321 Fourth, we found that NPY regulates *dbh* expression in the LC. Overexpression of NPY decreased
322 *dbh* mRNA level in the LC by 38% at 3 hours after heat shock in *Tg(hsp:npy)* larvae compared to
323 WT siblings ($P<0.05$, two-tailed Student's *t* test) (**Figures 7A and 7D**). This time point coincides

with the maximal effect of NPY overexpression on locomotor activity and sleep (**Figures 1A and 1C**), suggesting that NPY overexpression-induced sleep may result from reduced *dbh* expression, and thus reduced NE levels. However, effects of NPY overexpression on behavior begin within the first hour after heat shock, and we only observed a trend of decreased *dbh* mRNA at 1 and 2 hours after heat shock that did not reach statistical significance (**Figure 7D**). These observations suggest that reduced *dbh* expression may not be the primary cause of NPY overexpression-induced sleep, but may rather be a secondary effect that supports and maintains NPY-induced sleep, perhaps resulting from decreased LC neuron activity. We also tested whether NPY overexpression affects the level of *tyrosine hydroxylase* (*th*), which acts upstream of *dbh* in the NE synthesis pathway, in LC neurons. We found that NPY overexpression did not significantly change *th* mRNA level in the LC at 1, 2 or 3 hours after heat shock (data not shown). Reduced *dbh* expression is not simply a consequence of increased sleep, as *dbh* mRNA level was unaffected following overexpression of prokineticin 2 (Prok2) (**Figure 7E**), which has sleep-promoting effects similar to that of NPY overexpression [68]. Treatment of WT larvae with the sedative melatonin also did not affect *dbh* mRNA level (**Figure 7E**). The interaction between NPY and *dbh* appears to be specific, as NPY overexpression did not affect expression of other genes involved in promoting arousal, including the neuropeptides *hypocretin* (*hcrt*) [20, 48] or *adenylate cyclase activating polypeptide 1a* (*adcyap1a*) (Singh and Prober, unpublished) (**Figures 7B, 7C and 7E**). These results indicate that overexpression of NPY selectively decreases the level of *dbh* mRNA in the LC, presumably resulting in decreased NE levels and thus increased sleep. In support of this finding, we observed that *dbh* mRNA level was 33% higher in the LC of *npy*-/- larvae compared to their *npy*+/- and *npy*+/+ siblings during the day (**Figures 7F and 7G**) ($P<0.05$, one-way ANOVA, Holm-Sidak test). Moreover, we found that *dbh* mRNA level in the LC of WT larvae was 25% lower at night compared to the day ($P<0.05$, two-tailed Student's *t* test) (**Figures 7H**). This result demonstrates a correlation between the wake circadian phase of this diurnal species and the level of *dbh* mRNA in the LC, and suggests that changes in NE levels contribute

to the regulation of normal sleep/wake states. Taken together, these results are consistent with a model in which NPY promotes sleep by inhibiting NE signaling.

DISCUSSION

Using a genetic screening strategy to identify neuropeptides that regulate vertebrate sleep, here we show that NPY regulates sleep in the zebrafish, a diurnal vertebrate. Previous rodent studies using infusion of NPY peptide resulted in either increased [31-37] or decreased [40-42] sleep. In agreement with some of these studies, intravenous injection of NPY was shown to promote sleep in both young healthy men [38] and depressed human patients [39]. The opposite observed effects of NPY infusion may have resulted from different sites of injection or dosage, or the use of *in vitro* synthesized NPY peptide that may lack modifications present on endogenously produced peptide. These studies may also be confounded by extensive interactions between mechanisms that regulate sleep and other functions of NPY. Indeed, wake-promoting effects of injected NPY were associated with feeding-like behaviors in rats [40-42]. Central administration of NPY in rodents has also been shown to induce hypothermia [69] and to increase social interactions [70], which may affect sleep. Correlative studies have documented reduced NPY levels in patients with major depression who report sleep disturbances [71] and in Chinese patients with primary insomnia [72], consistent with a role for endogenous NPY in promoting sleep. Lower NPY levels are also found in individuals with post-traumatic stress disorder (PTSD) who have insomnia and fragmented sleep [73, 74]. Additional studies have implicated *npy*-expressing neurons in mammalian sleep. For example, GABAergic cortical interneurons co-expressing *neuronal nitric oxide synthase* (*nnos*) and *npy* express *c-fos*, a marker of neuronal activity, during sleep in rodents [75]. Furthermore, extracellular single-unit activity in the basal forebrain of anaesthetized rats showed increased firing of *npy*-expressing neurons during slow wave sleep [76].

To address the role of endogenous NPY in sleep, we performed genetic gain- and loss-of-function studies using zebrafish larvae. These studies are performed before the onset of feeding, during which time larvae receive nutrients from the yolk sac [77], and before the onset of social interactions [78]. Furthermore, because zebrafish are poikilothermic, thermoregulation is unlikely to be a factor in studies of zebrafish sleep. Thus, zebrafish larvae allow the role of NPY in sleep to be addressed without complications of mammalian models. We found that overexpression of NPY suppresses locomotor activity and increases sleep during the day and night, whereas *npy* mutant zebrafish exhibit increased locomotor activity and decreased sleep during the day. Analysis of sleep architecture revealed that NPY overexpression results in shorter wake bouts, whereas *npy* mutants have longer wake bouts, suggesting that NPY regulates consolidation of the wake state. Consistent with this phenotype, we found that chemogenetic ablation of *npy*-expressing neurons resulted in decreased sleep during the day, again due to longer wake bouts. The specificity of the loss-of-function phenotype to the day could be explained by the presence of redundant sleep-promoting systems at night, the primary sleep phase of zebrafish. Consistent with our observations, overexpression in *Drosophila* of neuropeptide F (NPF), a *Drosophila* homolog of NPY, or its receptor NPFR1, promotes sleep, although knockdown experiments did not show a sleep phenotype [79]. The *Drosophila* short neuropeptide F (sNPF), which is unrelated to NPF [80], is also thought to promote sleep [81] and has been referred to as an NPY ortholog, but is more likely an ortholog of vertebrate RFamide related peptides [80]. In *C. elegans*, locomotor quiescence during the developmentally regulated lethargus sleep state is abolished in mutants lacking the receptor *npr-1* and reduced in mutants lacking the *npr-1* ligands *flp-18* and *flp-21* [82]. *npr-1* mutants also show increased responsiveness to oxygen and pheromones, resulting in altered foraging and accelerated locomotion [83-85]. While NPR-1 is structurally related to mammalian NPY receptors [86], FLP-18 and FLP-21 appear to be more similar to the RFamide family of peptides [80, 87]. Combined with our results, these studies establish NPY as a conserved sleep promoting neuropeptide in both vertebrates and invertebrates, and the

correlative human studies described above suggest that this function may be conserved in humans.

npy is widely expressed in the mammalian brain, particularly in the hypothalamus, amygdala, LC and cerebral cortex [50, 51]. Similar to mammals, NPY is expressed in several discrete brain regions in zebrafish larvae. Because of this broad expression pattern, NPY could act via several known sleep/wake regulators. First, *npy*-expressing neurons innervate *hcrt*-expressing neurons in the hypothalamus, and application of NPY reduces spike frequency and hyperpolarizes *hcrt* neurons in mouse hypothalamic slices [88]. Second, a hypothalamic population of *npy*-expressing neurons project to the histaminergic tuberomammillary nucleus (TMN) in rodents [89]. Third, corticotropin releasing hormone (CRH) impairs sleep and enhances vigilance [90], and NPY enhances inhibitory synaptic transmission in *crh*-expressing neurons in amygdala brain slices [91]. Fourth, exogenous melatonin promotes sleep in diurnal vertebrates, including humans [92], and application of NPY to rat pineal explants increases melatonin production [93]. To determine whether any of these pathways underlie the sleep-promoting effects of NPY, we tested whether the NPY overexpression phenotype is blocked in zebrafish mutants in which these pathways are affected. We found that the NPY overexpression phenotype persisted in larvae lacking Hcrt signaling, histamine, CRH or melatonin using animals containing mutations in the *hcrt receptor*, *hdc*, *crha*, *crhb* or *aanat2*, respectively. We also found that NPY overexpression increased sleep in WT and melatonin-treated animals to a similar extent. These observations suggest that NPY does not affect sleep by modulating these pathways.

In contrast to these negative results, we made several observations suggesting that NPY promotes sleep by inhibiting NE signaling. Both pharmacological and genetic studies in mammals and zebrafish have shown that NE promotes arousal [48, 64, 65]. We previously showed that both genetic and pharmacological inhibition of NE signaling increases sleep in zebrafish larvae [48].

Here we found that although overexpression of NPY increases sleep in *dbh*+/- larvae and DMSO-treated WT larvae, it does not enhance the increased sleep observed in *dbh*-/- larvae and prazosin-treated WT larvae. These results suggest that NPY overexpression promotes sleep by inhibiting NE signaling. Consistent with this possibility, we found that treatment with prazosin abolished the decreased sleep observed in *npy* mutants, suggesting that elevated NE signaling underlies this phenotype. In support of these functional interactions, we found that NPY overexpression decreases the level of *dbh* mRNA in the LC, the primary source of NE in the brain [65], and thus likely reduces NE levels. We observed a trend of reduced *dbh* mRNA levels at 1 and 2 hours after induction of NPY overexpression that did not reach statistical significance, and a significant reduction at 3 hours post-heat shock. These observations suggest that reduced *dbh* expression may not be the primary cause of NPY overexpression-induced sleep, but rather may be a secondary effect that supports and maintains NPY-induced sleep, perhaps resulting from decreased LC neuron activity. Consistent with this possibility, *in vitro* synthesized NPY can inhibit LC neurons in rodent brain slices [94]. However, we observed the maximal effect of NPY overexpression on locomotor activity and sleep at ~3 hours after heat shock, coinciding with a significant reduction in *dbh* mRNA level in the LC, suggesting that NPY may directly promote sleep by decreasing *dbh* expression, and thus NE production, in the LC. Moreover, we found that *npy* mutants had higher *dbh* mRNA levels in the LC compared to sibling controls, presumably resulting in increased NE levels and increased wakefulness. It was recently shown that *dbh* levels in whole zebrafish larvae undergo a circadian oscillation [95]. Consistent with this observation, we found that the level of *dbh* mRNA in the LC is lower at night compared to the day, suggesting that NE levels may contribute to the diurnal sleep/wake cycle.

Consistent with an interaction between NPY and the LC, we identified a small population of *npy*-expressing neurons that is adjacent to, and appears to innervate, the LC. This observation contrasts with mammals, where *npy* and *dbh* are co-expressed in LC neurons [96, 97]. We were

unable to detect expression of NPY receptors in LC neurons, suggesting that NPY may indirectly affect NE signaling. However, expression of GPCRs, the protein class of NPY receptors, is notoriously difficult to detect, and we thus cannot rule out the possibility that a NPY receptor is expressed in LC neurons. We did observe expression of *npyr1* and *npyr2l* in cells near the LC, suggesting the possibility of local indirect interactions between NPY neurons and the LC. Thus, while the anatomic interaction between the NPY and NE systems appears to differ in zebrafish and mammals, the functional relationship between the systems may be conserved. Taken together, these observations suggest that NPY could regulate sleep by directly affecting the firing of LC neurons and/or the level of NE. Alternately, the relevant site of action for the interaction between NPY and NE in sleep may lie in a network of neurons near the LC or elsewhere in the brain.

In both mammals and zebrafish, NE signaling plays a key role in mediating the wake-promoting functions of Hcrt signaling and *hcrt*-expressing neurons [47, 48]. Here we provide evidence that NE signaling mediates the sedating effect of NPY, suggesting a central role for the NE system in neuropeptidergic regulation of sleep/wake states. Interestingly, while Hcrt and NPY have opposite effects on sleep via NE signaling, both neuropeptides promote feeding via neuronal substrates in the hypothalamus [30, 98], suggesting a segregation of neuronal circuits that mediate the effects of these neuropeptides on sleep and feeding. While an interaction between NPY and the LC has been shown to control stress responses in rodents [99], to our knowledge this is the first demonstration of an interaction between NPY and the NE system in the context of sleep.

Recently the therapeutic potential of NPY has been demonstrated due to its ability to promote recovery after traumatic experiences for individuals with PTSD. Cerebrospinal fluid levels of NPY are reduced in individuals suffering from PTSD who have sleep disturbances [74]. Interestingly, treatment with prazosin substantially reduces nightmares and improves sleep in these patients

[74]. Since we found that NPY overexpression reduces the level of *dbh* mRNA, and presumably NE, the lower level of NPY in PTSD might result in increased NE levels, thereby disrupting sleep. Moreover, *npy* mutant mice exhibit anxiety-like symptoms that could result from a hyperactive LC [44, 100], suggesting that comorbidity of anxiety and sleep disturbances could result from this interaction.

In summary, our results identify NPY as a regulator of sleep/wake behaviors in the zebrafish and suggest that NPY promotes sleep by inhibiting NE signaling. These results highlight a central role for NE signaling in regulating sleep, and suggest that modulation of NPY signaling may be a useful therapeutic approach for sleep disorders.

AUTHOR CONTRIBUTIONS

DAP and JR performed the genetic screen. CS and DAP conceptualized and designed the experiments, and generated reagents. CS performed the experiments and analyzed the data. CS and DAP wrote the paper with assistance from JR. DAP supervised the project.

ACKNOWLEDGMENTS

We thank Daisy Chilin, Alex Mack Cruz, Axel Dominguez and Kenna Molinder for animal husbandry assistance, Viveca Sapin and Uyen Pham for genotyping assistance, Owen Randlett, Ulrich Herget, Caroline Wee, and Marcus Ghosh for assistance with Z-brain registration, and Grigorios Oikonomou for comments on the manuscript. This work was supported by grants from the NIH (DAP: NS070911, NS101665, NS095824, NS101158), the Mallinckrodt, Rita Allen and Brain and Behavior Research Foundations (DAP), and a UCL Excellence Fellowship and European Research Council Starting Grant (JR). We declare no conflicts of interest.

STAR Methods

Contact for Reagent and Resource Sharing

Further information and requests for reagents may be directed to, and will be fulfilled by, the Lead Contact David A. Prober (dprober@caltech.edu).

Experimental Model and Subject Details

Zebrafish experiments and husbandry followed standard protocols [101] in accordance with Caltech Institutional Animal Care and Use Committee guidelines. Larval zebrafish were studied before the onset of sexual differentiation and all behavioral experiments were performed using siblings with the same genetic background, differing only in the presence of a transgene, mutation of a specific gene, or treatment with drugs and appropriate vehicle controls. The age of animals used in each experiment is described in the manuscript, in each figure legend, and/or in the STAR Methods.

Transgenic and mutant zebrafish

Tg(hsp:npy) ct853Tg. Full-length zebrafish *npy* cDNA was isolated using 5' and 3' RACE (FirstChoice RLM-RACE, AM1700, Thermo Fisher Scientific) and the open reading frame was cloned downstream of the zebrafish *hsp70c* promoter [20] in a vector containing flanking I-SceI endonuclease recognition sites. The same zebrafish *npy* gene was cloned in a previous study [102], but the gene isolated in our study contains an arginine residue located C-terminal to the mature peptide domain that was reported as an alanine residue in the previous study [102]. The sequence reported in our study is the same as that reported by the zebrafish genome sequencing project (www.ensembl.org/Danio_rerio). The alanine residue described in the previous report [102] is therefore likely either a sequencing error or a polymorphism in the fish strain used**.** Stable transgenic lines were generated by injecting plasmids with I-SceI (R0694, New England Biolabs Inc.) into zebrafish embryos at the one-cell stage. Transgenic founders were identified by outcrossing potential founders, heat shocking progeny at 5 dpf, fixing animals 30 minutes after

heat shock and performing ISH using an *npy*-specific probe. *Tg(hsp:npy)* fish were genotyped using the primers 5'-CCGCCACCATGAATCCA-3' and 5'-GGTTTGTCCAAACTCATCAATGT-3', which generate a 370 bp band. We generated two independent *Tg(hsp:npy)* stable transgenic lines that produced similar phenotypes, but all data shown in the paper are from the line that produced stronger phenotypes.

npy mutant ct811. *npy* mutant zebrafish were generated using the zinc finger nuclease method [56]. The mutant contains a 17 bp deletion (AGCCCGACAACCCGGGA) after nucleotide 94 of the open reading frame, resulting in a translational frame shift beginning at the fourth amino acid of the mature peptide domain. Mutant animals were genotyped using the primers 5'-ATAAATTGCGCATCAGCACA-3' and 5'-TGAGGAAGAATTTGAGACTACGC-3', which produce a 281 or 264 bp band for the WT or mutant allele, respectively. *npy* heterozygous mutants were outcrossed to the parental TLAB strain for four generations before use in behavioral experiments. Homozygous *npy* mutants are viable, fertile, lack obvious developmental defects and are morphologically indistinguishable from WT animals.

Tg(npy:kalta4) ct852Tg. We used bacterial artificial chromosome (BAC) recombineering [59] to insert an optimized version of the transcriptional activator Gal4 (KalTA4) [59] at the *npy* start codon of a BAC (zK50N10SP6; HUKGB735N1050Q, Source BioScience)) containing 288 kb of genomic sequence, including 145 kb upstream and 143 kb downstream of the *npy* gene. Primers of 70 nucleotides (pIndigoBAC_HA1_iTol2_F and pIndigoBAC_HA1_iTol2_R, **Table S3**) were used to amplify the long terminal repeats of the medaka Tol2 transposon to enable single-copy integration of the BAC into the zebrafish genome, using the plasmid *pIndigoBAC-536* [59] as template. *npy*-specific primers were designed that contain 50 nucleotide homology arms around the *npy* start codon (positions -53 to -4 and +4 to +53) with ~20 nucleotide ends (Homology arm F and Homology arm R, **Table S3** to amplify a KalTA4_kanamycin cassette from the plasmid

pCS2+_kalta4_kanR [59]. These plasmids were a kind gift from Dr. Stefan Schulte-Merker. The modified BAC was purified using the Nucleobond BAC 100 kit (740579, Macherey-Nagel) and injected into zebrafish embryos at the one- or two-cell stage at a concentration of 50 ng/µL, along with *tol2 transposase* mRNA at a concentration of 50 ng/µL. Transgenic lines were identified by mating potential founders to WT TLAB fish, and progeny were genotyped using the primers 5'-CGCTATCATTTATAGATTTTTGCAC-3' and 5'-AGTAGCGACACTCCCAGTTG-3', which produce a 220 bp band in transgenic animals. Transgenic founders were crossed to the *Tg(uas:nfsb-mcherry)* line [60] and the strongest line was identified by fluorescence microscopy.

Other transgenic and mutant lines. The *Tg(dbh:EGFP)* transgenic line [67], *dbh* mutant [48], *hcrtr* mutant [19], *hdc* mutant [62], and *aanat2* mutant [63] have been previously described. The *crha* and *crhb* mutants are unpublished (Singh and Prober unpublished).

Method Details

Locomotor activity assay. At 4 dpf, individual larvae were placed into each well of a 96-well plate (7701-1651, GE Healthcare Life Sciences) containing 650 µL of E3 embryo medium (5 mM NaCl, 0.17 mM KCl, 0.33 mM $CaCl_2$, 0.33 mM $MgSO_4$, pH 7.4). Plates were sealed with an optical adhesive film (4311971, Applied Biosystems) to prevent evaporation, except in experiments where drugs were added. The sealing process introduces air bubbles in some wells, which are excluded from analysis. In experiments using transgenic animals, larvae were blindly assigned a position in the plate, and were genotyped after the behavioral experiment was completed. Locomotor activity was monitored using an automated videotracking system (Viewpoint Life Sciences) with a Dinion one-third inch monochrome camera (Dragonfly 2, Point Grey) fitted with a fixed-angle megapixel lens (M5018-MP, Computar) and infrared filter. For heat shock-induced overexpression experiments, larvae were heat shocked at 37°C for 1 hour starting at either 3 p.m. or 10 p.m. at 5 dpf. The movement of each larva was captured at 15 Hz and recorded using the

584 quantization mode in 1-minute time bins. The 96-well plate and camera were housed inside a
585 custom-modified Zebrabox (Viewpoint Life Sciences) that was continuously illuminated with
586 infrared LEDs, and illuminated with white LEDs from 9 a.m. to 11 p.m., except as noted in constant
587 light or constant dark experiments. The 96-well plate was housed in a chamber filled with
588 recirculating water to maintain a constant temperature of 28.5°C. The parameters used for
589 detection were: detection threshold, 15; burst, 29; freeze, 3, which were determined empirically.
590 Data were processed using custom PERL and Matlab (The Mathworks, Inc.) scripts, and
591 statistical tests were performed using Prism 6 (GraphPad).
592
593 A movement was defined as a pixel displacement between adjacent video frames preceded and
594 followed by a period of inactivity of at least 67 ms (the limit of temporal resolution). Any one-
595 minute period with no movement was defined as one minute of sleep based on arousal threshold
596 changes [20]. A sleep bout was defined as a continuous string of sleep minutes. Average activity
597 was defined as the average amount of activity in seconds/hour, including sleep bouts.
598
599 Arousal threshold assay. The arousal threshold assay was performed as described [48]. Animals
600 were heat shocked at 5 dpf from 12 p.m. to 1 p.m, and taps of 14 different intensities were applied
601 in a random order from 3 p.m. to 10 p.m. Thirty trials were performed at each stimulus intensity,
602 with a 1-minute inter-trial interval. The background probability of movement was calculated by
603 identifying for each genotype the fraction of larvae that moved 5 seconds prior to all stimuli
604 delivered. This value was subtracted from the average response fraction value for each tap event.
605 A response is defined as any movement that occurred within 1 second after a tap was delivered.
606 Data was analyzed using Matlab (Mathworks, Inc.) and dose-response curves were constructed
607 using the Variable Slope log(dose) response curve fitting module of Prism (Graphpad) and fitted
608 using ordinary least squares. The effective tap power 50 (ETP_{50}) was defined as the tapping

intensity at which 50% of the maximum number of responding larvae occurs, based on the fitted curve.

Tapping experiments with a 5-minute inter-trial interval were performed using three tap intensities of 2.3, 3.0 and 4.0 arbitrary units to assess the response of awake and sleeping larvae to the stimuli. These stimulus intensities were chosen because they were lower than the ETP_{50} of animals of both genotypes. Animals were heat shocked at 5 dpf from 12 p.m. to 1 p.m., and thirty-three trials were performed at each stimulus intensity in a random order from 3:00 p.m. to 10:30 p.m. Behavioral responses were analyzed as described above. Three independent experiments for were performed for both 1-minute and 5-minute tapping assays, and one representative experiment for each is shown.

In situ hybridization (ISH). Animals were fixed in 4% paraformaldehyde (PFA) in phosphate buffered saline (PBS) for 16 hours at room temperature. ISH was performed using digoxygenin (DIG) labeled antisense riboprobes (DIG RNA Labeling Kit, 11175025910, Sigma-Aldrich), followed by incubation with a sheep anti-digoxigenin-POD antibody (1:400; 11207733910, Sigma-Aldrich), and developed using the TSA Plus Fluorescein and Cyanine 3 System (NEL753001KT, PerkinElmer). Double-fluorescent ISH was performed using DIG- and fluorescein-labeled riboprobes (Fluorescein RNA Labeling kit, 11685619910, Sigma-Aldrich), and the TSA Plus Fluorescein and Cyanine 3 System (NEL753001KT, PerkinElmer) using a previously described protocol [20]. Probes specific for *npy*, *dbh*, *adcyap1a*, *kalta4*, *npyr1*, *npyr2*, *npyr2l*, *npyr4*, *npyr7*, *npyr8a* and *npyr8b* were synthesized using standard protocols [103]. The *npy* probe was transcribed using a PCR product amplified from a zebrafish cDNA library using the primers Forward: 5'-CCACAGAGCAAGAATTCCAA-3' and Reverse: 5'-CAGTCATTATTGTTCTCCTTTGC-3', and then serially amplified with the same Forward primer and the Reverse Primer with a T7 promoter sequence added: 5'-

TAATACGACTCACTATAGGGCAGTCATTATTGTTCTCCTTTGC-3'. The *kalta4* probe was transcribed using the plasmid *pCS2+_kalta4_kanR* [59] as a template after linearization with BamH1 and using T7 RNA polymerase (10881767001, Sigma-Aldrich). A probe specific for *dbh* has been previously described [104]. Probes specific for *adcyap1a*, *npyr1*, *npyr2*, *npyr2l*, *npyr4*, *npyr7*, *npyr8a* and *npyr8b* were generated as described for the *npy*-specific probe using the primers listed in **Table S3**.

Immunohistochemistry (IHC). Samples were fixed in 4% PFA in PBS overnight at 4°C and then washed with 0.25% Triton X-100/PBS (PBTx). Brains were manually dissected and blocked for at least 1 hour in 2% goat serum/2% dimethyl sulfoxide (DMSO)/PBTx at room temperature or overnight at 4°C. Primary antibody incubations were performed in blocking solution overnight at 4°C using chicken anti-GFP (1:400, GFP-1020, Aves Labs, Inc.) and rabbit anti-DsRed (1:100, 632496, Clontech Laboratories, Inc.). Secondary antibody incubations were performed in blocking solution overnight at 4°C using Alexa Fluor 488 goat anti-chicken (1:500, A-11039, Thermo Fisher Scientific) and Alexa Fluor 568 goat anti-rabbit (1:500, A-11011, Thermo Fisher Scientific) antibodies. Samples were mounted in 50% glycerol/PBS and imaged using a Zeiss LSM 780 confocal microscope with a 25x 0.8 NA water immersion objective (LD LCI Plan-Apochromat 25x/0.8 1mm Corr DIC M27). Images were processed using Fiji [105].

Z-brain registration. WT larvae were fixed at 6 dpf and ISH was performed using an *npy*-specific probe on dissected brains as described above, followed by IHC using mouse anti-t-ERK primary antibody (1:500, 4696, Cell Signaling Technology) and Alexa Fluor 488 goat anti-mouse secondary antibody (1:500, A32723, Thermo Fisher Scientific). Imaging was performed using a Zeiss 780 confocal microscope, using a 20x 1.0 NA water dipping objective (W Plan-Apochromat 20x/1.0 DIC CG=0.17 M27 75mm) and imaged at ~0.8/0.8/2 µm voxel size (x/y/z) using the Zeiss tiling function and the pairwise stitching function of Fiji [105]. Non-rigid image registration was

performed using the Computational Morphometry Toolkit (CMTK, http://www.nitrc.org/projects/cmtk/) as previously described [52]. t-ERK staining was used to register to the t-ERK reference brain [52], which was then used to align *npy* ISH labeling. Registered brains were analyzed using the Z-Brain browser (MATLAB) [52] to identify anatomical regions expressing *npy*. Using Fiji, the registered brain showing *npy* expression was merged to the database 'Anti-tERK_6dpf_MeanImageOf193Fish' from 'AnatomyLabel DatabaseDownsampled' from the Z-Brain Downloads [52] to show the expression of *npy* relative to t-ERK in the reference 6 dpf zebrafish larva. The combined stack was converted into a video and processed in Windows Movie Maker to add anatomical labels.

Image processing in Imaris and Fiji. Surface rendering to reconstruct projections of *npy*- and *dbh*-expressing neurons was performed using Imaris 9 (Bitplane). To perform surface rendering, we used the Volume function followed by the Normal Shading mode to add a depth effect to the 2-dimensional z-stack imaged using a 63x 1.4 NA oil immersion objective (Plan-Apochromat 63x/1.4 oil DIC M27), and then displayed the image in the 3-dimensional isometric view. We then used the Interactive Software Histogram to select a threshold that included as much of the neuronal projections as possible while excluding any background. Areas of overlap between projections from *npy*- and *dbh*-expressing neurons were magnified 4-fold and saved as TIFF images.

To identify the sources of overlapping projections, a 63x z-stack of *npy*-expressing and *dbh*-expressing neurons was converted to an 8-bit stack. Projections from a single *npy*-expressing neuron and a single *dbh*-expressing neuron were manually traced using the Simple Neurite Tracer plugin in Fiji. Tracings were then filled-in using the same plugin, with an exemplar *npy*-expressing neuron labeled magenta and an exemplar *dbh*-expressing neuron labeled green, and saved as individual z-stacks. These z-stacks were then merged with the original z-stack to so that the traced *npy*-expressing and *dbh*-expressing neurons were overlaid on the original images. As a result,

687 the traced *npy*-expressing neuron appears magenta and the traced *dbh*-expressing neuron
688 appears yellow. This merged image stack is shown in **Video S2**.
689
690 TUNEL staining. *Tg(npy:kalta4);Tg(uas:nfsb-mcherry*) larvae were treated with DMSO or 10 mM
691 MTZ for 18 hours starting at 3 dpf, and then were fixed in 4% PFA in PBS for 16 hours at 4°C,
692 and subjected to a TUNEL Assay (*In Situ* Cell Death Detection Kit, 11684795910, Sigma-Aldrich)
693 according to the manufacturer's instructions.
694
695 Analysis and quantification of *dbh* expression using ISH. *dbh* ISH was performed by incubating
696 fixed 5 dpf brains with a DIG-labeled *dbh* antisense riboprobe, followed by a sheep anti-
697 digoxigenin-POD antibody (1:400; 11207733910, Sigma-Aldrich), and developed using the TSA
698 Plus Cyanine 3 System (NEL753001KT, PerkinElmer). Samples were developed using the
699 cyanine 3 substrate at 1:300 for 5 minutes to avoid saturation. Brains were imaged using a Zeiss
700 LSM 780 confocal microscope using a 561 nm laser and a 25x 0.8 NA water immersion objective
701 (LD LCI Plan-Apochromat 25x/0.8 1mm Corr DIC M27). To quantify *dbh* expression in
702 *Tg(hsp:npy)* animals, larvae were heat shocked from 3 p.m. to 4 p.m. and samples were collected
703 at the indicated times after heat shock. To quantify *dbh* expression in *npy* mutants, samples were
704 collected at 4 p.m. Both experiments used siblings whose brains were processed for ISH in the
705 same tube, imaged, quantified and then genotyped by PCR. To compare *dbh* expression levels
706 during the day and night, day samples were collected at 4 p.m. and night samples were collected
707 at 2 a.m. After fixation, a small nick was made in the forebrain of night samples to enable their
708 identification at the end of the experiment. Day and night samples were then placed together in
709 the same tube, processed for ISH, imaged and then quantified. Three independent experiments
710 were performed and images of representative samples are shown. For quantification of *dbh*
711 mRNA level, confocal z-stacks were obtained as described above. Using Fiji [105], each z-stack
712 was converted into a maximum intensity projection, converted into 8-bit grayscale, and

713 thresholded to select only the fluorescent ISH signal. This function was applied to all images in
714 an experiment to determine a threshold level that was optimal for most images, and this threshold
715 was then used for all images in an experiment. The Analyze-Set Measurements function was
716 used to select Integrated Density as the measurement parameter and Limit to Threshold was
717 selected to measure only the thresholded region. Fluorescent intensity was then measured by the
718 Analyze-Measure function.
719
720 **Statistical Analysis**
721 All line graphs show a 1 hour forward moving average plotted in 10 minute bins, except **Figures**
722 **S1B and S1E**, which show data plotted in 10 minute bins. Line and bar graphs show mean ±
723 standard error of the mean (SEM). In all statistical tests, the significance threshold was set to
724 $P<0.05$. Parametric statistical tests were used because the data followed an approximately
725 normal distribution. For behavioral experiments that compared two genotypes, statistical
726 significance was assessed using a two-tailed Student's *t* test. For *npy* mutant experiments, which
727 compared animals of three different genotypes, one-way ANOVA followed by the Holm-Sidak
728 correction for multiple comparisons was performed to test for significant pair-wise comparisons
729 among all genotypes. The Holm-Sidak test was used to focus on significance but not confidence
730 intervals. For experiments in which NPY was overexpressed in various mutant backgrounds or in
731 which NPY overexpression was combined with drug treatments, statistical significance was
732 assessed using two-way ANOVA followed by the Holm-Sidak correction for multiple comparisons.
733 For experiments in which *npy* mutants were treated with drugs, statistical significance was
734 assessed using two-way ANOVA followed by Holm-Sidak correction for multiple comparisons.
735 For quantification of ISH data, statistical significance was assessed using a two-tailed Student's
736 *t* test for experiments that compared two samples, and one-way ANOVA followed by the Holm-
737 Sidak correction for multiple comparisons for experiments that compared three or more samples.
738 Behavioral data was processed using Matlab (MathWorks), graphs were generated using Excel

(Microsoft), and statistical analyses were performed using Prism 6 (Graphpad). The number of animals and statistical test used are stated in each figure or figure legend.

Data and Software Availability

Custom PERL and MATLAB code used for zebrafish behavioral analysis is available upon request.

REFERENCES

1. Richter, C., Woods, I.G., and Schier, A.F. (2014). Neuropeptidergic control of sleep and wakefulness. Annu Rev Neurosci *37*, 503-531.
2. Adamantidis, A.R., Zhang, F., Aravanis, A.M., Deisseroth, K., and de Lecea, L. (2007). Neural substrates of awakening probed with optogenetic control of hypocretin neurons. Nature *450*, 420-424.
3. de Lecea, L., Kilduff, T.S., Peyron, C., Gao, X., Foye, P.E., Danielson, P.E., Fukuhara, C., Battenberg, E.L., Gautvik, V.T., Bartlett, F.S., 2nd, et al. (1998). The hypocretins: hypothalamus-specific peptides with neuroexcitatory activity. Proc Natl Acad Sci U S A *95*, 322-327.
4. Lin, L., Faraco, J., Li, R., Kadotani, H., Rogers, W., Lin, X., Qiu, X., de Jong, P.J., Nishino, S., and Mignot, E. (1999). The sleep disorder canine narcolepsy is caused by a mutation in the hypocretin (orexin) receptor 2 gene. Cell *98*, 365-376.
5. Saper, C.B., Fuller, P.M., Pedersen, N.P., Lu, J., and Scammell, T.E. (2010). Sleep state switching. Neuron *68*, 1023-1042.
6. Sherin, J.E., Elmquist, J.K., Torrealba, F., and Saper, C.B. (1998). Innervation of histaminergic tuberomammillary neurons by GABAergic and galaninergic neurons in the ventrolateral preoptic nucleus of the rat. J Neurosci *18*, 4705-4721.
7. Sherin, J.E., Shiromani, P.J., McCarley, R.W., and Saper, C.B. (1996). Activation of ventrolateral preoptic neurons during sleep. Science *271*, 216-219.
8. Woods, I.G., Schoppik, D., Shi, V.J., Zimmerman, S., Coleman, H.A., Greenwood, J., Soucy, E.R., and Schier, A.F. (2014). Neuropeptidergic signaling partitions arousal behaviors in zebrafish. J Neurosci *34*, 3142-3160.
9. Konadhode, R.R., Pelluru, D., Blanco-Centurion, C., Zayachkivsky, A., Liu, M., Uhde, T., Glen, W.B., Jr., van den Pol, A.N., Mulholland, P.J., and Shiromani, P.J. (2013). Optogenetic stimulation of MCH neurons increases sleep. J Neurosci *33*, 10257-10263.

10. Tsunematsu, T., Ueno, T., Tabuchi, S., Inutsuka, A., Tanaka, K.F., Hasuwa, H., Kilduff, T.S., Terao, A., and Yamanaka, A. (2014). Optogenetic manipulation of activity and temporally controlled cell-specific ablation reveal a role for MCH neurons in sleep/wake regulation. J Neurosci *34*, 6896-6909.

11. Verret, L., Goutagny, R., Fort, P., Cagnon, L., Salvert, D., Leger, L., Boissard, R., Salin, P., Peyron, C., and Luppi, P.H. (2003). A role of melanin-concentrating hormone producing neurons in the central regulation of paradoxical sleep. BMC Neurosci *4*, 19.

12. Willie, J.T., Sinton, C.M., Maratos-Flier, E., and Yanagisawa, M. (2008). Abnormal response of melanin-concentrating hormone deficient mice to fasting: hyperactivity and rapid eye movement sleep suppression. Neuroscience *156*, 819-829.

13. Funato, H., Miyoshi, C., Fujiyama, T., Kanda, T., Sato, M., Wang, Z., Ma, J., Nakane, S., Tomita, J., Ikkyu, A., et al. (2016). Forward-genetics analysis of sleep in randomly mutagenized mice. Nature *539*, 378-383.

14. Shaw, P.J., Cirelli, C., Greenspan, R.J., and Tononi, G. (2000). Correlates of sleep and waking in Drosophila melanogaster. Science *287*, 1834-1837.

15. Hendricks, J.C., Finn, S.M., Panckeri, K.A., Chavkin, J., Williams, J.A., Sehgal, A., and Pack, A.I. (2000). Rest in Drosophila is a sleep-like state. Neuron *25*, 129-138.

16. Raizen, D.M., Zimmerman, J.E., Maycock, M.H., Ta, U.D., You, Y.J., Sundaram, M.V., and Pack, A.I. (2008). Lethargus is a Caenorhabditis elegans sleep-like state. Nature *451*, 569-572.

17. Van Buskirk, C., and Sternberg, P.W. (2007). Epidermal growth factor signaling induces behavioral quiescence in Caenorhabditis elegans. Nat Neurosci *10*, 1300-1307.

18. Zhdanova, I.V., Wang, S.Y., Leclair, O.U., and Danilova, N.P. (2001). Melatonin promotes sleep-like state in zebrafish. Brain Res *903*, 263-268.

19. Yokogawa, T., Marin, W., Faraco, J., Pezeron, G., Appelbaum, L., Zhang, J., Rosa, F., Mourrain, P., and Mignot, E. (2007). Characterization of sleep in zebrafish and insomnia in hypocretin receptor mutants. PLoS Biol *5*, e277.

20. Prober, D.A., Rihel, J., Onah, A.A., Sung, R.J., and Schier, A.F. (2006). Hypocretin/orexin overexpression induces an insomnia-like phenotype in zebrafish. J Neurosci *26*, 13400-13410.

21. Faraco, J.H., Appelbaum, L., Marin, W., Gaus, S.E., Mourrain, P., and Mignot, E. (2006). Regulation of hypocretin (orexin) expression in embryonic zebrafish. J Biol Chem *281*, 29753-29761.

22. Renier, C., Faraco, J.H., Bourgin, P., Motley, T., Bonaventure, P., Rosa, F., and Mignot, E. (2007). Genomic and functional conservation of sedative-hypnotic targets in the zebrafish. Pharmacogenet Genomics *17*, 237-253.

23. Kaslin, J., Nystedt, J.M., Ostergard, M., Peitsaro, N., and Panula, P. (2004). The orexin/hypocretin system in zebrafish is connected to the aminergic and cholinergic systems. J Neurosci *24*, 2678-2689.

24. Rihel, J., Prober, D.A., Arvanites, A., Lam, K., Zimmerman, S., Jang, S., Haggarty, S.J., Kokel, D., Rubin, L.L., Peterson, R.T., et al. (2010). Zebrafish behavioral profiling links drugs to biological targets and rest/wake regulation. Science *327*, 348-351.

25. Chiu, C.N., Rihel, J., Lee, D.A., Singh, C., Mosser, E.A., Chen, S., Sapin, V., Pham, U., Engle, J., Niles, B.J., et al. (2016). A Zebrafish Genetic Screen Identifies Neuromedin U as a Regulator of Sleep/Wake States. Neuron *89*, 842-856.

26. Alfalah, M., and Michel, M.C. (2004). Neuropeptide Y and related peptides, (Berlin ; New York: Springer).

27. Beck, B. (2006). Neuropeptide Y in normal eating and in genetic and dietary-induced obesity. Philos Trans R Soc Lond B Biol Sci *361*, 1159-1185.

28. Sohn, J.W., Elmquist, J.K., and Williams, K.W. (2013). Neuronal circuits that regulate feeding behavior and metabolism. Trends Neurosci *36*, 504-512.

29. Yulyaningsih, E., Zhang, L., Herzog, H., and Sainsbury, A. (2011). NPY receptors as potential targets for anti-obesity drug development. Br J Pharmacol *163*, 1170-1202.

30. Zeltser, L.M., Seeley, R.J., and Tschop, M.H. (2012). Synaptic plasticity in neuronal circuits regulating energy balance. Nat Neurosci *15*, 1336-1342.

31. Akanmu, M.A., Ukponmwan, O.E., Katayama, Y., and Honda, K. (2006). Neuropeptide-Y Y2-receptor agonist, PYY3-36 promotes non-rapid eye movement sleep in rat. Neurosci Res *54*, 165-170.

32. Fuxe, K., Agnati, L.F., Harfstrand, A., Zini, I., Tatemoto, K., Pich, E.M., Hokfelt, T., Mutt, V., and Terenius, L. (1983). Central administration of neuropeptide Y induces hypotension bradypnea and EEG synchronization in the rat. Acta Physiol Scand *118*, 189-192.

33. Heilig, M., and Murison, R. (1987). Intracerebroventricular neuropeptide Y suppresses open field and home cage activity in the rat. Regul Pept *19*, 221-231.

34. Jolicoeur, F.B., Michaud, J.N., Rivest, R., Menard, D., Gaudin, D., Fournier, A., and St-Pierre, S. (1991). Neurobehavioral profile of neuropeptide Y. Brain Res Bull *26*, 265-268.

35. Naveilhan, P., Canals, J.M., Valjakka, A., Vartiainen, J., Arenas, E., and Ernfors, P. (2001). Neuropeptide Y alters sedation through a hypothalamic Y1-mediated mechanism. Eur J Neurosci *13*, 2241-2246.

36. Toth, A., Hajnik, T., Zaborszky, L., and Detari, L. (2007). Effect of basal forebrain neuropeptide Y administration on sleep and spontaneous behavior in freely moving rats. Brain Res Bull *72*, 293-301.

37. Zini, I., Merlo Pich, E., Fuxe, K., Lenzi, P.L., Agnati, L.F., Harfstrand, A., Mutt, V., Tatemoto, K., and Moscara, M. (1984). Actions of centrally administered neuropeptide Y on EEG activity in different rat strains and in different phases of their circadian cycle. Acta Physiol Scand *122*, 71-77.

38. Antonijevic, I.A., Murck, H., Bohlhalter, S., Frieboes, R.M., Holsboer, F., and Steiger, A. (2000). Neuropeptide Y promotes sleep and inhibits ACTH and cortisol release in young men. Neuropharmacology *39*, 1474-1481.

39. Held, K., Antonijevic, I., Murck, H., Kuenzel, H., and Steiger, A. (2006). Neuropeptide Y (NPY) shortens sleep latency but does not suppress ACTH and cortisol in depressed patients and normal controls. Psychoneuroendocrinology *31*, 100-107.

40. Stanley, B.G., and Leibowitz, S.F. (1984). Neuropeptide Y: stimulation of feeding and drinking by injection into the paraventricular nucleus. Life Sci *35*, 2635-2642.

41. Szentirmai, E., and Krueger, J.M. (2006). Central administration of neuropeptide Y induces wakefulness in rats. Am J Physiol Regul Integr Comp Physiol *291*, R473-480.

42. Ushimura, A., Tsuji, T., Tanaka, S., Kogo, M., and Yamamoto, T. (2015). Neuropeptide-Y modulates eating patterns and masticatory muscle activity in rats. Behav Brain Res *278*, 520-526.

43. Brown, J.A., Woodworth, H.L., and Leinninger, G.M. (2015). To ingest or rest? Specialized roles of lateral hypothalamic area neurons in coordinating energy balance. Frontiers in systems neuroscience *9*, 9.

44. Bannon, A.W., Seda, J., Carmouche, M., Francis, J.M., Norman, M.H., Karbon, B., and McCaleb, M.L. (2000). Behavioral characterization of neuropeptide Y knockout mice. Brain Res *868*, 79-87.

45. Reichmann, F., Wegerer, V., Jain, P., Mayerhofer, R., Hassan, A.M., Frohlich, E.E., Bock, E., Pritz, E., Herzog, H., Holzer, P., et al. (2016). Environmental enrichment induces behavioural disturbances in neuropeptide Y knockout mice. Sci Rep *6*, 28182.

46. Patel, H.R., Qi, Y., Hawkins, E.J., Hileman, S.M., Elmquist, J.K., Imai, Y., and Ahima, R.S. (2006). Neuropeptide Y deficiency attenuates responses to fasting and high-fat diet in obesity-prone mice. Diabetes *55*, 3091-3098.

47. Carter, M.E., Brill, J., Bonnavion, P., Huguenard, J.R., Huerta, R., and de Lecea, L. (2012). Mechanism for Hypocretin-mediated sleep-to-wake transitions. Proc Natl Acad Sci U S A *109*, E2635-2644.

48. Singh, C., Oikonomou, G., and Prober, D.A. (2015). Norepinephrine is required to promote wakefulness and for hypocretin-induced arousal in zebrafish. Elife *4*, e07000.

49. Lamesch, P., Li, N., Milstein, S., Fan, C., Hao, T., Szabo, G., Hu, Z., Venkatesan, K., Bethel, G., Martin, P., et al. (2007). hORFeome v3.1: a resource of human open reading frames representing over 10,000 human genes. Genomics *89*, 307-315.

50. Chronwall, B.M., DiMaggio, D.A., Massari, V.J., Pickel, V.M., Ruggiero, D.A., and O'Donohue, T.L. (1985). The anatomy of neuropeptide-Y-containing neurons in rat brain. Neuroscience *15*, 1159-1181.

51. Dumont, Y., Martel, J.C., Fournier, A., St-Pierre, S., and Quirion, R. (1992). Neuropeptide Y and neuropeptide Y receptor subtypes in brain and peripheral tissues. Prog Neurobiol *38*, 125-167.

52. Randlett, O., Wee, C.L., Naumann, E.A., Nnaemeka, O., Schoppik, D., Fitzgerald, J.E., Portugues, R., Lacoste, A.M., Riegler, C., Engert, F., et al. (2015). Whole-brain activity mapping onto a zebrafish brain atlas. Nat Methods *12*, 1039-1046.

53. Cavanaugh, D.J., Vigderman, A.S., Dean, T., Garbe, D.S., and Sehgal, A. (2016). The Drosophila Circadian Clock Gates Sleep through Time-of-Day Dependent Modulation of Sleep-Promoting Neurons. Sleep *39*, 345-356.

54. Mrosovsky, N. (1999). Masking: history, definitions, and measurement. Chronobiol Int *16*, 415-429.

55. Siegel, J.M. (2009). Sleep viewed as a state of adaptive inactivity. Nat Rev Neurosci *10*, 747-753.

56. Chen, S., Oikonomou, G., Chiu, C.N., Niles, B.J., Liu, J., Lee, D.A., Antoshechkin, I., and Prober, D.A. (2013). A large-scale in vivo analysis reveals that TALENs are significantly

897 more mutagenic than ZFNs generated using context-dependent assembly. Nucleic Acids
898 Res *41*, 2769-2778.
899 57. Albers, H.E., and Ferris, C.F. (1984). Neuropeptide Y: role in light-dark cycle entrainment
900 of hamster circadian rhythms. Neurosci Lett *50*, 163-168.
901 58. Huhman, K.L., Gillespie, C.F., Marvel, C.L., and Albers, H.E. (1996). Neuropeptide Y
902 phase shifts circadian rhythms in vivo via a Y2 receptor. Neuroreport *7*, 1249-1252.
903 59. Bussmann, J., and Schulte-Merker, S. (2011). Rapid BAC selection for tol2-mediated
904 transgenesis in zebrafish. Development *138*, 4327-4332.
905 60. Davison, J.M., Akitake, C.M., Goll, M.G., Rhee, J.M., Gosse, N., Baier, H., Halpern, M.E.,
906 Leach, S.D., and Parsons, M.J. (2007). Transactivation from Gal4-VP16 transgenic
907 insertions for tissue-specific cell labeling and ablation in zebrafish. Dev Biol *304*, 811-824.
908 61. Curado, S., Anderson, R.M., Jungblut, B., Mumm, J., Schroeter, E., and Stainier, D.Y.
909 (2007). Conditional targeted cell ablation in zebrafish: a new tool for regeneration studies.
910 Dev Dyn *236*, 1025-1035.
911 62. Chen, A., Singh, C., Oikonomou, G., and Prober, D.A. (2017). Genetic Analysis of
912 Histamine Signaling in Larval Zebrafish Sleep. eNeuro *4*.
913 63. Gandhi, A.V., Mosser, E.A., Oikonomou, G., and Prober, D.A. (2015). Melatonin is
914 required for the circadian regulation of sleep. Neuron *85*, 1193-1199.
915 64. Berridge, C.W., Schmeichel, B.E., and Espana, R.A. (2012). Noradrenergic modulation of
916 wakefulness/arousal. Sleep Med Rev *16*, 187-197.
917 65. Berridge, C.W., and Waterhouse, B.D. (2003). The locus coeruleus-noradrenergic system:
918 modulation of behavioral state and state-dependent cognitive processes. Brain Res Brain
919 Res Rev *42*, 33-84.
920 66. Sundstrom, G., Larsson, T.A., Xu, B., Heldin, J., and Larhammar, D. (2013). Interactions
921 of zebrafish peptide YYb with the neuropeptide Y-family receptors Y4, Y7, Y8a, and Y8b.
922 Front Neurosci *7*, 29.

67. Liu, J., Merkle, F.T., Gandhi, A.V., Gagnon, J.A., Woods, I.G., Chiu, C.N., Shimogori, T., Schier, A.F., and Prober, D.A. (2015). Evolutionarily conserved regulation of hypocretin neuron specification by Lhx9. Development *142*, 1113-1124.

68. Chen, S., Reichert, S., Singh, C., Oikonomou, G., Rihel, J., and Prober, D.A. (2017). Light-Dependent Regulation of Sleep and Wake States by Prokineticin 2 in Zebrafish. Neuron *95*, 153-168 e156.

69. Esteban, J., Chover, A.J., Sanchez, P.A., Mico, J.A., and Gibert-Rahola, J. (1989). Central administration of neuropeptide Y induces hypothermia in mice. Possible interaction with central noradrenergic systems. Life Sci *45*, 2395-2400.

70. Sajdyk, T.J., Johnson, P.L., Leitermann, R.J., Fitz, S.D., Dietrich, A., Morin, M., Gehlert, D.R., Urban, J.H., and Shekhar, A. (2008). Neuropeptide Y in the amygdala induces long-term resilience to stress-induced reductions in social responses but not hypothalamic-adrenal-pituitary axis activity or hyperthermia. J Neurosci *28*, 893-903.

71. Gjerris, A., Widerlov, E., Werdelin, L., and Ekman, R. (1992). Cerebrospinal fluid concentrations of neuropeptide Y in depressed patients and in controls. J Psychiatry Neurosci *17*, 23-27.

72. Huang, Q., Liao, J., Liu, Y., Liang, H., Ma, P., and Pan, J. (2015). Plasma neuropeptide Y levels in Chinese patients with primary insomnia. Sleep Breath *19*, 617-622.

73. Germain, A., Buysse, D.J., and Nofzinger, E. (2008). Sleep-specific mechanisms underlying posttraumatic stress disorder: integrative review and neurobiological hypotheses. Sleep Med Rev *12*, 185-195.

74. Raskind, M.A., Peskind, E.R., Hoff, D.J., Hart, K.L., Holmes, H.A., Warren, D., Shofer, J., O'Connell, J., Taylor, F., Gross, C., et al. (2007). A parallel group placebo controlled study of prazosin for trauma nightmares and sleep disturbance in combat veterans with post-traumatic stress disorder. Biol Psychiatry *61*, 928-934.

948 75. Gerashchenko, D., Wisor, J.P., Burns, D., Reh, R.K., Shiromani, P.J., Sakurai, T., de la
949 Iglesia, H.O., and Kilduff, T.S. (2008). Identification of a population of sleep-active cerebral
950 cortex neurons. Proc Natl Acad Sci U S A *105*, 10227-10232.
951 76. Duque, A., Balatoni, B., Detari, L., and Zaborszky, L. (2000). EEG correlation of the
952 discharge properties of identified neurons in the basal forebrain. J Neurophysiol *84*, 1627-
953 1635.
954 77. Clift, D., Richendrfer, H., Thorn, R.J., Colwill, R.M., and Creton, R. (2014). High-
955 throughput analysis of behavior in zebrafish larvae: effects of feeding. Zebrafish *11*, 455-
956 461.
957 78. Dreosti, E., Lopes, G., Kampff, A.R., and Wilson, S.W. (2015). Development of social
958 behavior in young zebrafish. Front Neural Circuits *9*, 39.
959 79. He, C., Yang, Y., Zhang, M., Price, J.L., and Zhao, Z. (2013). Regulation of sleep by
960 neuropeptide Y-like system in Drosophila melanogaster. PLoS One *8*, e74237.
961 80. Nassel, D.R., and Wegener, C. (2011). A comparative review of short and long
962 neuropeptide F signaling in invertebrates: Any similarities to vertebrate neuropeptide Y
963 signaling? Peptides *32*, 1335-1355.
964 81. Shang, Y., Donelson, N.C., Vecsey, C.G., Guo, F., Rosbash, M., and Griffith, L.C. (2013).
965 Short neuropeptide F is a sleep-promoting inhibitory modulator. Neuron *80*, 171-183.
966 82. Choi, S., Chatzigeorgiou, M., Taylor, K.P., Schafer, W.R., and Kaplan, J.M. (2013).
967 Analysis of NPR-1 reveals a circuit mechanism for behavioral quiescence in C. elegans.
968 Neuron *78*, 869-880.
969 83. Cheung, B.H., Cohen, M., Rogers, C., Albayram, O., and de Bono, M. (2005). Experience-
970 dependent modulation of C. elegans behavior by ambient oxygen. Curr Biol *15*, 905-917.
971 84. Gray, J.M., Karow, D.S., Lu, H., Chang, A.J., Chang, J.S., Ellis, R.E., Marletta, M.A., and
972 Bargmann, C.I. (2004). Oxygen sensation and social feeding mediated by a C. elegans
973 guanylate cyclase homologue. Nature *430*, 317-322.

974 85. Macosko, E.Z., Pokala, N., Feinberg, E.H., Chalasani, S.H., Butcher, R.A., Clardy, J., and
975 Bargmann, C.I. (2009). A hub-and-spoke circuit drives pheromone attraction and social
976 behaviour in C. elegans. Nature *458*, 1171-1175.
977 86. de Bono, M., and Bargmann, C.I. (1998). Natural variation in a neuropeptide Y receptor
978 homolog modifies social behavior and food response in C. elegans. Cell *94*, 679-689.
979 87. Rogers, C., Reale, V., Kim, K., Chatwin, H., Li, C., Evans, P., and de Bono, M. (2003).
980 Inhibition of Caenorhabditis elegans social feeding by FMRFamide-related peptide
981 activation of NPR-1. Nat Neurosci *6*, 1178-1185.
982 88. Fu, L.Y., Acuna-Goycolea, C., and van den Pol, A.N. (2004). Neuropeptide Y inhibits
983 hypocretin/orexin neurons by multiple presynaptic and postsynaptic mechanisms: tonic
984 depression of the hypothalamic arousal system. J Neurosci *24*, 8741-8751.
985 89. Lee, E.Y., Hwang, Y.G., and Lee, H.S. (2016). Hypothalamic neuronal origin of
986 neuropeptide Y (NPY) or cocaine- and amphetamine-regulated transcript (CART) fibers
987 projecting to the tuberomammillary nucleus of the rat. Brain Res.
988 90. Steiger, A. (2002). Sleep and the hypothalamo-pituitary-adrenocortical system. Sleep Med
989 Rev *6*, 125-138.
990 91. Pleil, K.E., Rinker, J.A., Lowery-Gionta, E.G., Mazzone, C.M., McCall, N.M., Kendra, A.M.,
991 Olson, D.P., Lowell, B.B., Grant, K.A., Thiele, T.E., et al. (2015). NPY signaling inhibits
992 extended amygdala CRF neurons to suppress binge alcohol drinking. Nat Neurosci *18*,
993 545-552.
994 92. Brzezinski, A., Vangel, M.G., Wurtman, R.J., Norrie, G., Zhdanova, I., Ben-Shushan, A.,
995 and Ford, I. (2005). Effects of exogenous melatonin on sleep: a meta-analysis. Sleep Med
996 Rev *9*, 41-50.
997 93. Vacas, M.I., Sarmiento, M.I., Pereyra, E.N., Etchegoyen, G.S., and Cardinali, D.P. (1987).
998 In vitro effect of neuropeptide Y on melatonin and norepinephrine release in rat pineal
999 gland. Cell Mol Neurobiol *7*, 309-315.

94. Finta, E.P., Regenold, J.T., and Illes, P. (1992). Depression by neuropeptide Y of noradrenergic inhibitory postsynaptic potentials of locus coeruleus neurones. Naunyn Schmiedebergs Arch Pharmacol *346*, 472-474.

95. Huang, J., Zhong, Z., Wang, M., Chen, X., Tan, Y., Zhang, S., He, W., He, X., Huang, G., Lu, H., et al. (2015). Circadian modulation of dopamine levels and dopaminergic neuron development contributes to attention deficiency and hyperactive behavior. J Neurosci *35*, 2572-2587.

96. Gray, T.S., and Morley, J.E. (1986). Neuropeptide Y: anatomical distribution and possible function in mammalian nervous system. Life Sci *38*, 389-401.

97. Holets, V.R., Hokfelt, T., Rokaeus, A., Terenius, L., and Goldstein, M. (1988). Locus coeruleus neurons in the rat containing neuropeptide Y, tyrosine hydroxylase or galanin and their efferent projections to the spinal cord, cerebral cortex and hypothalamus. Neuroscience *24*, 893-906.

98. Inutsuka, A., and Yamanaka, A. (2013). The physiological role of orexin/hypocretin neurons in the regulation of sleep/wakefulness and neuroendocrine functions. Front Endocrinol (Lausanne) *4*, 18.

99. Zitnik, G.A. (2016). Control of arousal through neuropeptide afferents of the locus coeruleus. Brain Res *1641*, 338-350.

100. Karl, T., Duffy, L., and Herzog, H. (2008). Behavioural profile of a new mouse model for NPY deficiency. Eur J Neurosci *28*, 173-180.

101. Westerfield, M. (1993). The zebrafish book : a guide for the laboratory use of zebrafish (Brachydanio rerio) (Eugene, OR: M. Westerfield).

102. Soderberg, C., Wraith, A., Ringvall, M., Yan, Y.L., Postlethwait, J.H., Brodin, L., and Larhammar, D. (2000). Zebrafish genes for neuropeptide Y and peptide YY reveal origin by chromosome duplication from an ancestral gene linked to the homeobox cluster. J Neurochem *75*, 908-918.

103. Thisse, C., and Thisse, B. (2008). High-resolution in situ hybridization to whole-mount zebrafish embryos. Nat Protoc *3*, 59-69.

104. Guo, S., Brush, J., Teraoka, H., Goddard, A., Wilson, S.W., Mullins, M.C., and Rosenthal, A. (1999). Development of noradrenergic neurons in the zebrafish hindbrain requires BMP, FGF8, and the homeodomain protein soulless/Phox2a. Neuron *24*, 555-566.

105. Schindelin, J., Arganda-Carreras, I., Frise, E., Kaynig, V., Longair, M., Pietzsch, T., Preibisch, S., Rueden, C., Saalfeld, S., Schmid, B., et al. (2012). Fiji: an open-source platform for biological-image analysis. Nat Methods *9*, 676-682.

FIGURE LEGENDS

Figure 1. Overexpression of zebrafish NPY increases sleep and arousal threshold. (A-G) Overexpression of zebrafish NPY following a heat shock at 3 p.m. results in decreased locomotor activity (**A,B**) and increased sleep (**C,D**). Yellow bars in line graphs indicate time of heat shock (HS). NPY overexpression increased the number of sleep bouts (**E**) and decreased the length of both sleep bouts (**F**) and wake bouts (**G**). Pre-HS and Post-HS quantify data for day 5 before and after heat shock, respectively. Mean ± SEM from 4 pooled experiments is shown. (**H**) Representative stimulus-response curve for *Tg(hsp:npy)* animals compared to WT siblings following heat shock at 12 p.m. Each data point represents mean ± SEM. Dashed lines mark the ETP_{50} value for each genotype. *Tg(hsp:npy)* animals had an ETP_{50} value of 24.2 vs. 8.2 for WT siblings (293% increase, $P< 0.05$ by extra sum-of-squares F test). (**I,J**) Overexpression of NPY reduces the response of *Tg(hsp:npy)* animals to the stimulus compared to WT siblings during both awake and sleep states. Stimulus intensities of 2.3, 3.0 and 4.0 arbitrary units (a.u.) were tested. A dose-dependent response is observed for WT animals but not for their *Tg(hsp:npy)* siblings. Bar graphs show mean ± SEM. n=number of animals. **P*<0.05; ***P*<0.01; ****P*<0.001; *****P*<0.0001 by two-tailed Student's *t* test. *See also Figures S1 and S2*.

Figure 2. Loss of *npy* reduces daytime sleep. (**A**) Amino acid sequences of WT and mutant zebrafish NPY proteins. The mature peptide is indicated with a red box. The altered amino acids following the frameshift in the mutant are shaded grey. (**B-M**) *npy*-/- animals were more active (**B,C**), and slept less (**E,F**), than their *npy*+/+ and *npy*+/- siblings during the day. During the day, *npy*-/- animals had fewer sleep bouts (**H**), and longer wake bouts (**L**) than their *npy*+/+ and *npy*+/- siblings. Mean ± SEM from 7 pooled experiments is shown. n=number of animals. ***P*<0.01; ****P*<0.001; *****P*<0.0001 by one-way ANOVA with Holm-Sidak post hoc test.

Figure 3. Entrained *npy* mutants sleep less in constant light. Larvae were entrained in 14:10 hour LD cycles for the first 4 days and nights of development, then behaviorally monitored for 24 hours in LD and then for 48 hours in LL. *npy*-/- animals were more active (**A-C**) and slept less (**D-F**) than their *npy*+/- and *npy*+/+ siblings during subjective day and night. *npy*-/- animals had fewer (**G,H**) and shorter (**I,J**) sleep bouts, and longer wake bouts (**K,L**) than their *npy*+/- and *npy*+/+ siblings. Mean ± SEM from 3 pooled experiments is shown. n=number of animals. **P*<0.05; ***P*<0.01; ****P*<0.001; *****P*<0.0001 by one-way ANOVA with Holm-Sidak post hoc test. *See also Figure S3*.

Figure 4. Loss of *npy*-expressing neurons reduces daytime sleep. (**A**) Ventral views of brains from 5 dpf *Tg(npy:kalta4)*;*Tg(uas:nfsb-mcherry)* animals stained with anti-DsRed antibody following treatment with either DMSO (**A**) or 10 mM MTZ (**A'**), showing nearly complete loss of mCherry labeling after MTZ treatment**.** (**B**) Mean ± SEM mCherry fluorescence intensity for *Tg(npy:kalta4)*;*Tg(uas:nfsb-mcherry)* animals treated with DMSO (n=4) or MTZ (n=4). (**C-N**) *Tg(npy:kalta4)*;*Tg(uas:nfsb-mcherry)* animals treated with MTZ were more active (**C,D**) and slept less (**F,G**) than their identically treated *Tg(npy:kalta4)* siblings during the day. This phenotype was due to fewer sleep bouts (**I**) and longer wake bouts (**M**). Mean ± SEM from 3 pooled experiments is shown (**C-N**). n=number of animals. **P*<0.05; ***P*<0.01; *****P*<0.0001 by two-tailed Student's *t* test. *See also Figures S4, S5 and Table S1*.

Figure 5. Evidence for anatomical interaction between hindbrain NPY neurons and the locus coeruleus. (**A**) Double FISH using probes specific for *npy* and *dbh* show their close proximity in the LC. Boxed region in (**A"**) is shown at higher magnification in a 50 µm thick maximum intensity projection in (**B**). (**C**) *Tg(npy:kalta4)*;*Tg(uas:nfsb-mcherry)*;*Tg(dbh:EGFP)* brains labeled using anti-DsRed and anti-EGFP antibodies. Boxed region in (**C"**) is shown at higher magnification (25x) in (**D**) and (63x) in (**D'**). Maximum intensity projections 40 µm and 63

µm thick are shown in (**D**) and (**D'**), respectively. (**E**) Imaris surface renderings of the boxed region in (**D'**). Boxed regions are shown at higher magnification in (**F-H**). White asterisks show close proximity of projections from NPY and LC neurons. (**I-J**) ISH using *npyr1*- and *npyr2l*-specific probes and immunostaining using an anti-EGFP antibody in *Tg(dbh:EGFP)* brains reveal close proximity of *npyr1* (**I**) and *npyr2l* (**J**) to *dbh*-expressing LC neurons. (**I'**) and (**J'**) show orthogonal views of the 24 µm and 25 µm thick maximum intensity projections shown in (**I**) and (**J**), respectively. a, anterior; p, posterior. All samples are 5 dpf brains. Scale bar: (**A-C**) 50 µm, (**B,D**) 10 µm, (**D'**) 7.5 µm, (**E**) 2.0 µm and (**F-H**) 0.5 µm.

Figure 6. Functional evidence that NPY promotes sleep by inhibiting noradrenergic signaling. (**A-D**) The sedating effects of NPY overexpression and loss of NE signaling are not additive. *Tg(hsp:npy);dbh-/-* and *dbh-/-* animals were less active (**A,B**) and slept more (**C,D**) than their *dbh+/-* siblings during the day before and after heat shock. *Tg(hsp:npy);dbh+/-* animals were less active and slept more than their *dbh+/-* siblings during the day after heat shock. NPY overexpression in *Tg(hsp:npy);dbh-/-* animals did not further decrease locomotor activity or increase sleep compared to their *dbh-/-* siblings. Yellow bars in line graphs indicate time of heat shock (HS). Pre-HS and Post-HS quantify data before and after heat shock. (**E-J**) Treatment with prazosin abolishes the *npy* mutant activity and sleep phenotypes. *npy+/+*, *npy+/-* and *npy-/-* siblings were treated with either DMSO or prazosin. DMSO-treated *npy-/-* larvae were more active (**E,F**) and slept less (**H,I**) than their DMSO-treated *npy+/-* and *npy+/+* siblings during the day. Prazosin treatment decreased activity (**E,F**) and increased sleep (**H,I**) to a similar extent for *npy-/-*, *npy+/-* and *npy+/+* siblings. Arrows indicate behavioral artifacts due to addition of water to each well. Mean ± SEM for 2 (**A-D**) or 4 (**E-J**) pooled experiments is shown. n=number of animals. n.s.=not significant, **P*<0.05; ***P*<0.01; *****P*<0.0001 by two-way ANOVA with Holm-Sidak post hoc test. *See also Table S2 and Figures S6 and S7*.

Figure 7. NPY signaling affects *dbh* mRNA level in the LC. (**A**) ISH showing *dbh* expression in the LC (boxed) and medulla oblongata. *dbh* mRNA levels were lower in *Tg(hsp:npy)* animals (**A”**) compared to their WT siblings (**A’**) after heat shock. ISH using probes specific for *adcyap1a* (**B**) and *hcrt* (**C**). Boxed regions in (**A-C**) are quantified in (**D,E**). (**D**) *dbh* mRNA level in the LC is decreased in *Tg(hsp:npy)* animals compared to their WT siblings at 3 hours post HS, but there is no significant difference at 1, 2, or 7 hours post HS. (**E**) Overexpression of Prok2 or treatment with 20 µM melatonin did not affect *dbh* mRNA level. Overexpression of NPY did not affect *adcyap1a* or *hcrt* mRNA level. (**F-F’**) *dbh* mRNA level in the LC was higher in *npy-/-* animals (**F’**) compared to their *npy*+/+ siblings (**F**). (**G**) Quantification of *dbh* mRNA level in the LC of *npy-/-* larvae and their sibling controls. (**H**) *dbh* mRNA levels in the LC of WT larvae were lower at night compared to the day. Mean ± SEM integrated fluorescence pixel intensity from 8-12 brains for each condition is shown. **P*<0.05 by two-tailed Student’s *t* test (**D,H**) or by one-way ANOVA with Holm-Sidak post hoc test (**G**). a, anterior; p, posterior. All samples are 5 dpf brains. Scale bar: (**A,B,C**) 100 µm; (**A’,A’’,F,F’**) 10 µm.

KEY RESOURCES TABLE

REAGENT or RESOURCE	SOURCE	IDENTIFIER
Antibodies		
Chicken anti-GFP	Aves Labs, Inc.	Cat# GFP-1020; RRID: AB_10000240
Rabbit anti-DsRed	Clontech Laboratories, Inc.	Cat# 632496; RRID: AB_10013483
Mouse anti-Erk1/2 (t-ERK)	Cell Signaling Technology	Cat# 4696; RRID: AB_390780
Goat anti-chicken IgG secondary antibody, Alexa 488 conjugate	Thermo Fisher Scientific	Cat# A-11039; RRID: 2534096
Goat anti-rabbit IgG secondary antibody, Alexa 568 conjugate	Thermo Fisher Scientific	Cat# A-11011; RRID: AB_143157
Goat anti-mouse IgG secondary antibody, Alexa 488 conjugate	Thermo Fisher Scientific	Cat# A32723; RRID: AB_2633275
Sheep anti-Digoxigenin-POD, Fab fragments	Sigma-Aldrich	Cat# 11207733910; RRID: AB_514500
Sheep anti-Fluorescein-POD, Fab fragments	Sigma-Aldrich	Cat# 11426346910; RRID: AB_840257
Chemicals, Peptides, and Recombinant Proteins		
16% paraformaldehyde	Electron Microscopy Sciences	Cat# 15710
Normal goat serum	Thermo Fisher Scientific	Cat# 31873
Prazosin hydrochloride	Sigma-Aldrich	Cat# P7791
Melatonin	Sigma-Aldrich	Cat# M5250
Metronidazole	Sigma-Aldrich	Cat# 46461
Dimethyl sulfoxide	Macron Fine Chemicals	Cat# 4948
T7 RNA polymerase	Sigma-Aldrich	Cat# 10881767001
Blocking reagent	Sigma-Aldrich	Cat# 11096176001
Critical Commercial Assays		
DIG RNA Labeling Kit	Sigma-Aldrich	Cat# 11175025910
Fluorescein RNA Labeling Kit	Sigma-Aldrich	Cat# 11685619910
FirstChoice RLM-RACE	Thermo Fisher Scientific	Cat# AM1700
TSA Plus Cyanine 3 and Fluorescein System	PerkinElmer	Cat# NEL753001KT
NucleoBond BAC 100 purification kit	Macherey-Nagel	Cat# 740579
In Situ Cell Death Detection Kit, Fluorescein	Sigma-Aldrich	Cat# 11684795910
Experimental Models: Organisms/Strains		
Zebrafish: *Tg(hsp:npy)* ct853Tg	This paper	RRID: ZDB-ALT-171002-3
Zebrafish: *npy* ct811 mutant	[56]	RRID: ZDB-ALT-131125-18
Zebrafish: *Tg(npy:kalta4)* ct852Tg	This paper	RRID: ZDB-ALT-170927-8
Zebrafish: *Tg(uas:nfsb-mcherry)* ct264Tg	[60]	RRID: ZDB-ALT-070316-1
Zebrafish: *Tg(dbh:EGFP)* ct821Tg	[67]	RRID: ZDB-ALT-150605-3

Zebrafish: *aanat2* ct801 mutant	[63]	RRID: ZDB-ALT-131122-2
Zebrafish: *hcrtr* hu2098 mutant	[19]	RRID: ZDB-ALT-070427-14
Zebrafish: *hdc* ct836 mutant	[62]	RRID: ZDB-ALT-170509-2
Zebrafish: *crha* ct861 mutant	This paper	RRID: ZDB-ALT-171009-1
Zebrafish: *crhb* ct862 mutant	This paper	RRID: ZDB-ALT-171009-2
Oligonucleotides		
Primers for genotyping, see Table S3	This paper	N/A
Primers for riboprobe synthesis, see Table S3	This paper	N/A
Primers for BAC transgenesis, see Table S3	This paper	N/A
Recombinant DNA		
Tg(hsp:npy)	This paper	N/A
Tg(npy:kalta4) BAC	This paper	N/A
pIndigoBAC	[59]	N/A
pCS2+_kalta4_kanR	[59]	N/A
Software and Algorithms		
Excel	Microsoft	https://products.office.com/en-us/excel
Fiji	[105]	https://fiji.sc; RRID: SCR_002285
GraphPad Prism6	GraphPad Software	http://www.graphpad.com/; RRID: SCR_002798
MATLAB	MathWorks, Inc.	https://www.mathworks.com/products/matlab
Computational Morphometry Toolkit	NITRC	(CMTK, http://www.nitrc.org/projects/cmtk/)
Imaris 9	Bitplane	http://www.bitplane.com/imaris; RRID: SCR_007370
Other		
96-well plate for behavioral experiments	GE Healthcare Life Sciences	Cat# 7701-1651
MicroAmp Optical Adhesive Film	Thermo Fisher Scientific	Cat# 4311971
Plasmid for *hcrt* riboprobe synthesis	[20]	N/A
Plasmid for *dbh* riboprobe synthesis	[48]	N/A
Plasmid for *adcyap1a* riboprobe synthesis	This paper	N/A
Plasmid for *npy* riboprobe synthesis	This paper	N/A
BAC containing zebrafish *npy* locus	Source BioScience	zK50N10SP6 (HUKGB735N1050Q)

Figure 1. Overexpression of zebrafish NPY increases sleep and arousal threshold

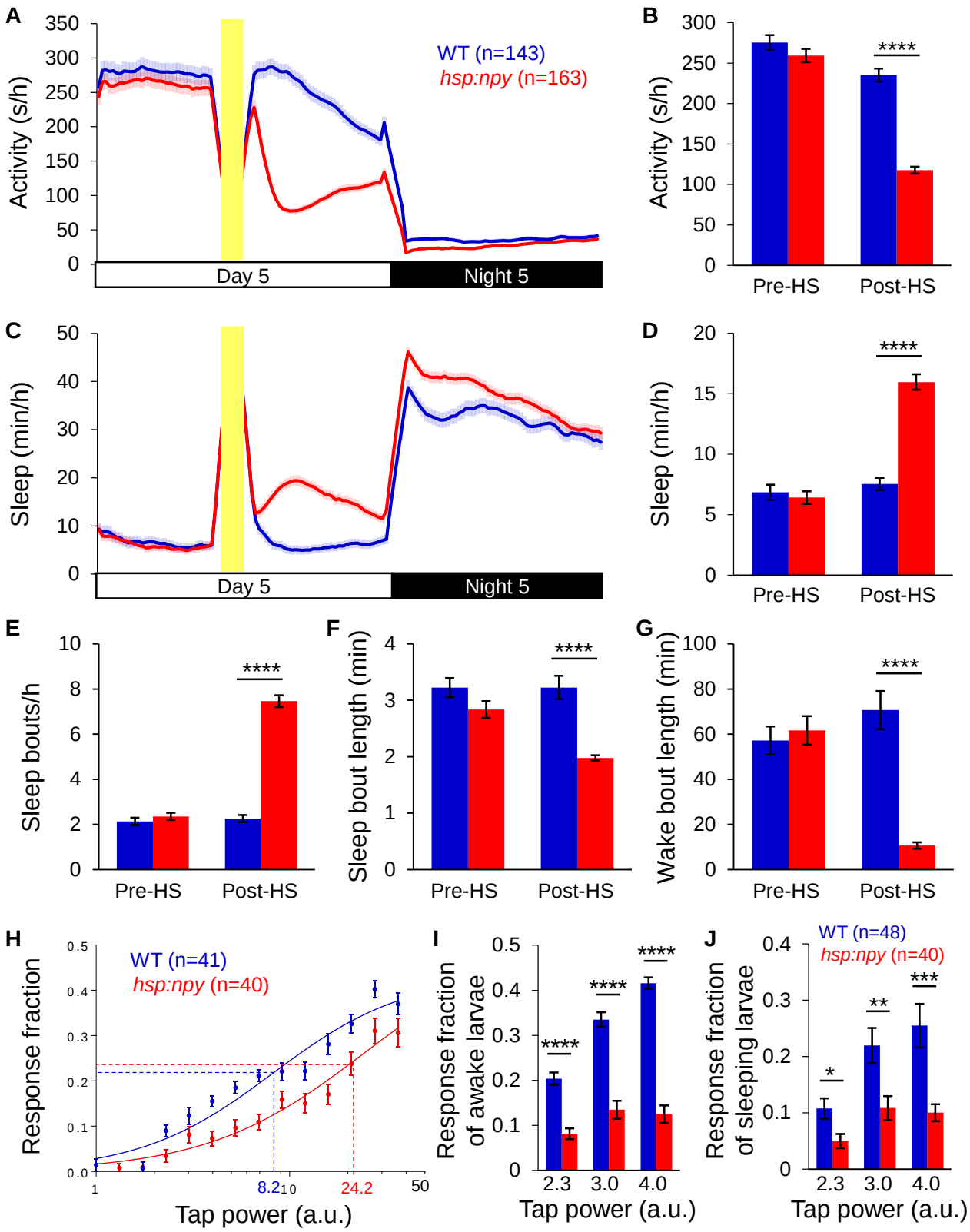

Figure 2. Loss of *npy* reduces daytime sleep

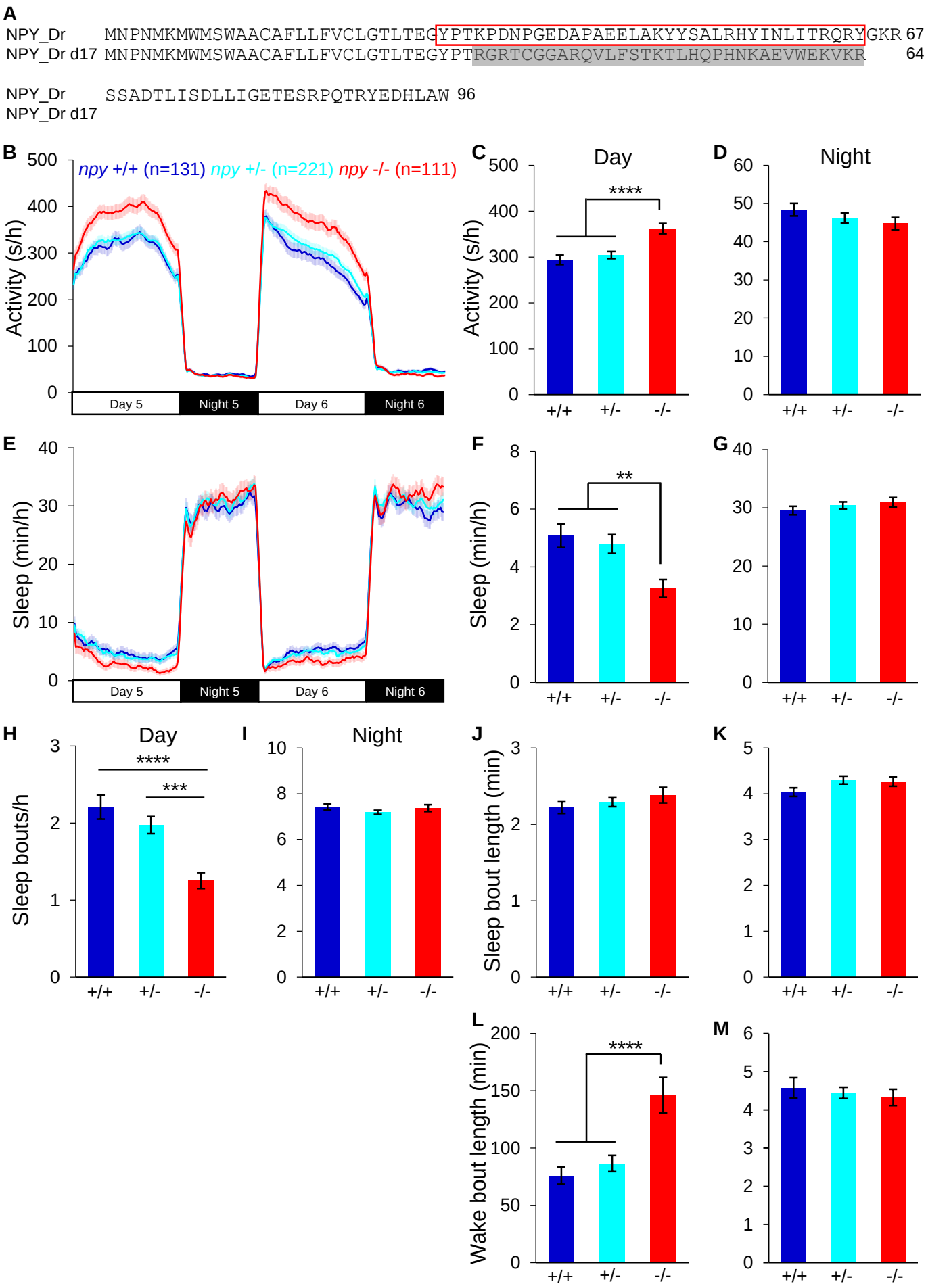

Figure 3. Entrained *npy* mutants sleep less in constant light

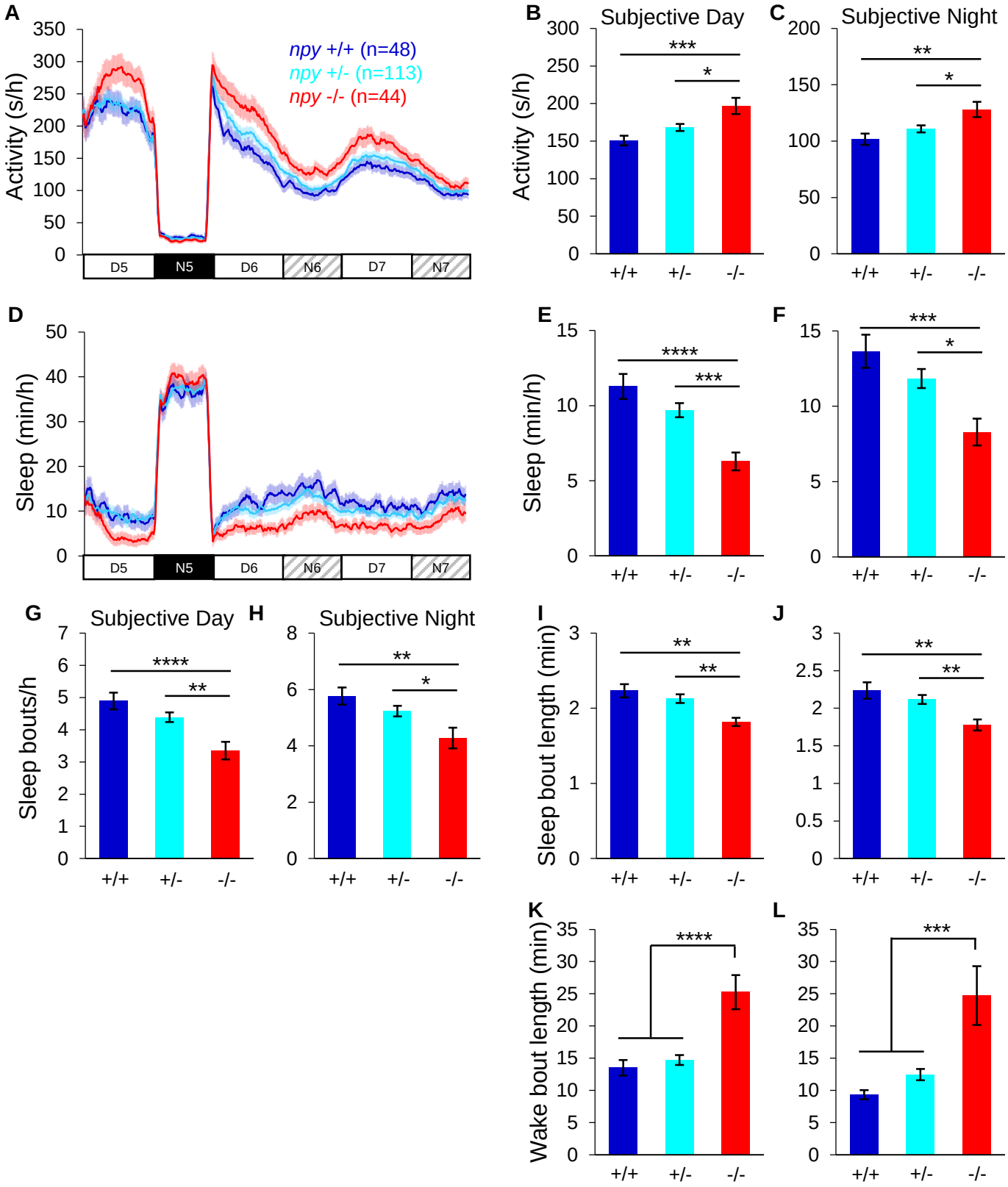

Figure 4. Loss of *npy*-expressing neurons reduces daytime sleep

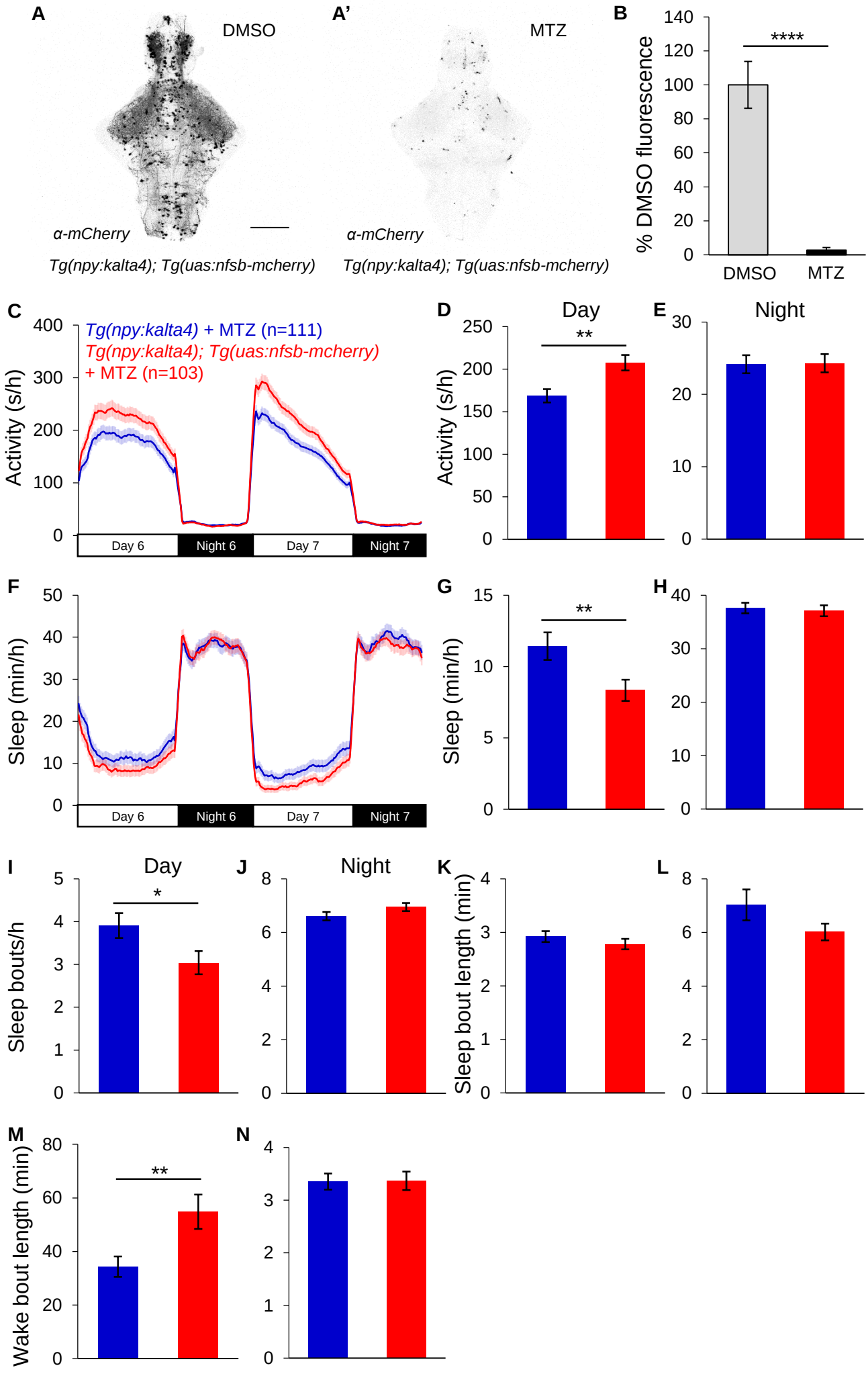

Figure 5. Evidence for anatomical interaction between NPY-positive and locus coeruleus

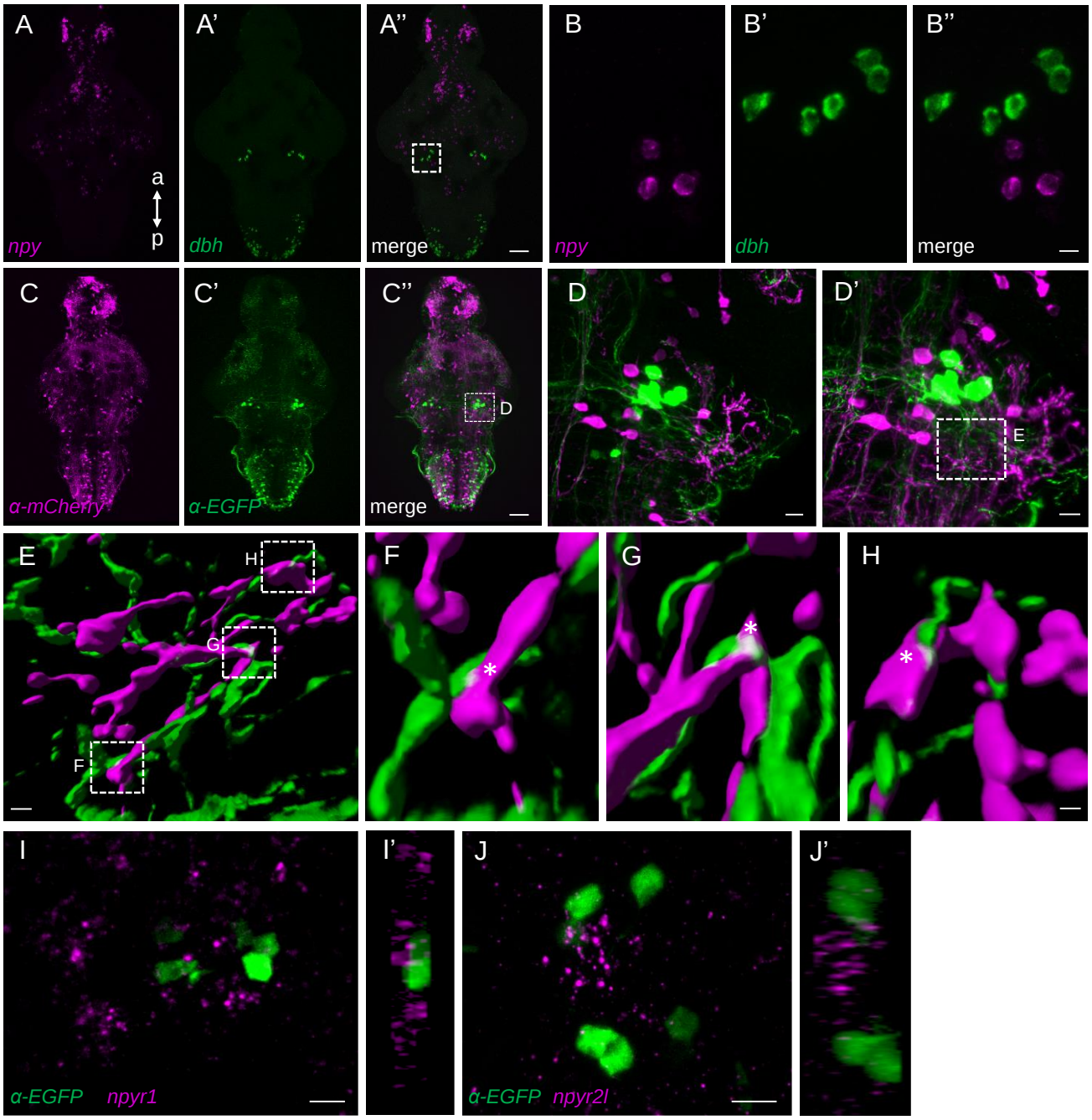

Figure 6. Functional evidence that NPY promotes sleep by inhibiting noradrenergic signaling

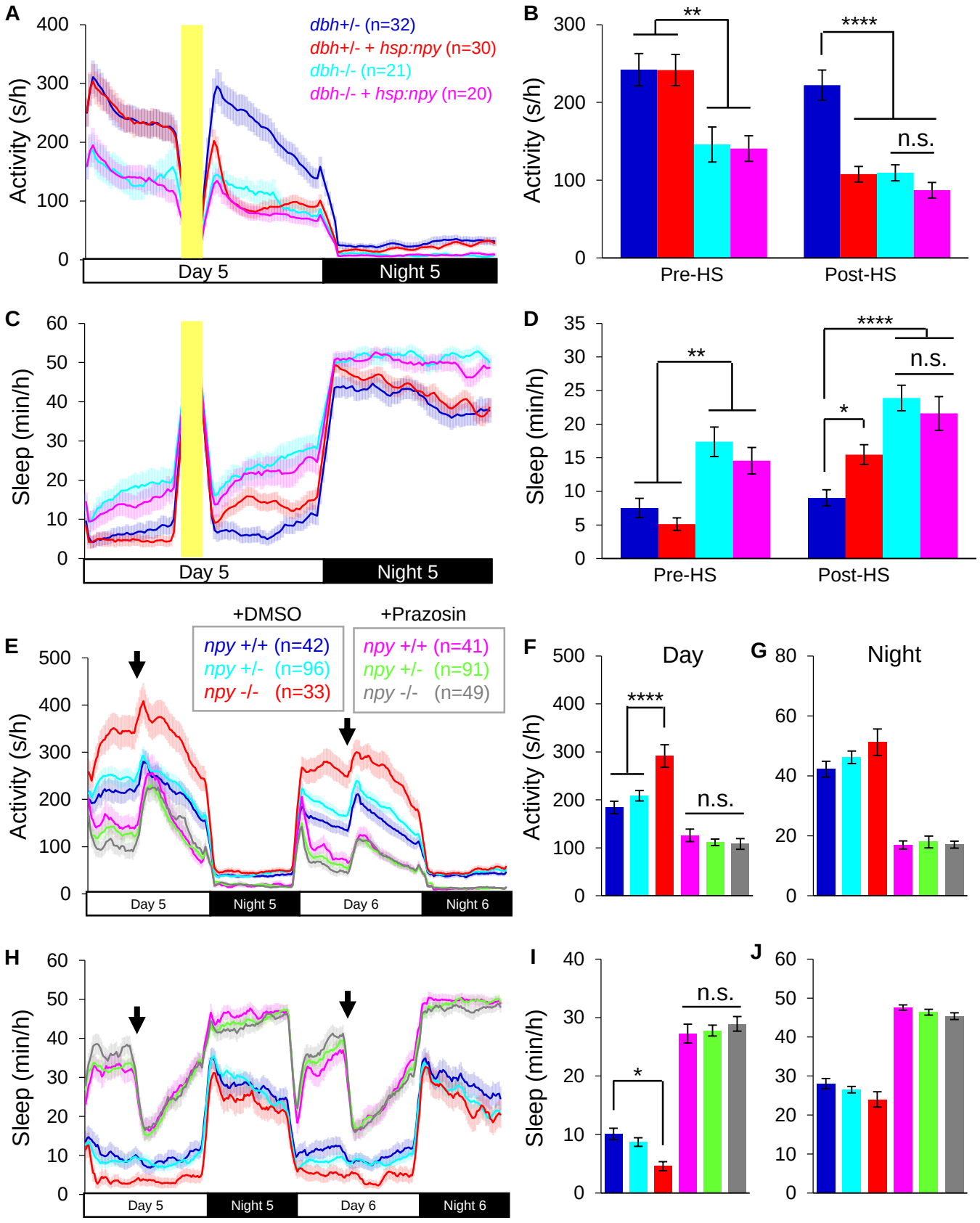

Figure 7. NPY signaling affects *dbh* mRNA level in the LC

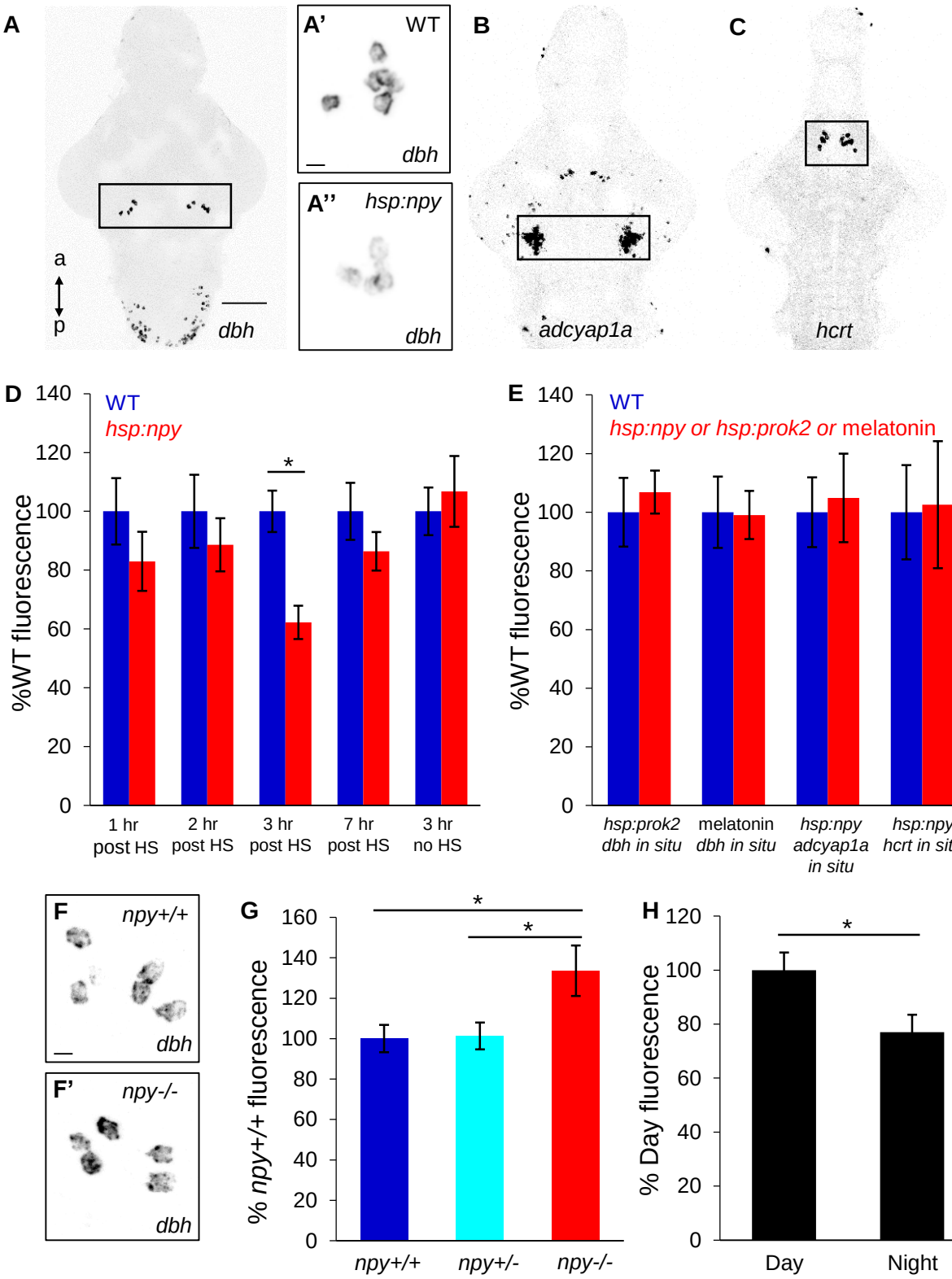

Figure S1. A genetic screen identifies a sleep-promoting role for NPY and zebrafish *npy* is widely expressed in the brain (Related to Figure 1)

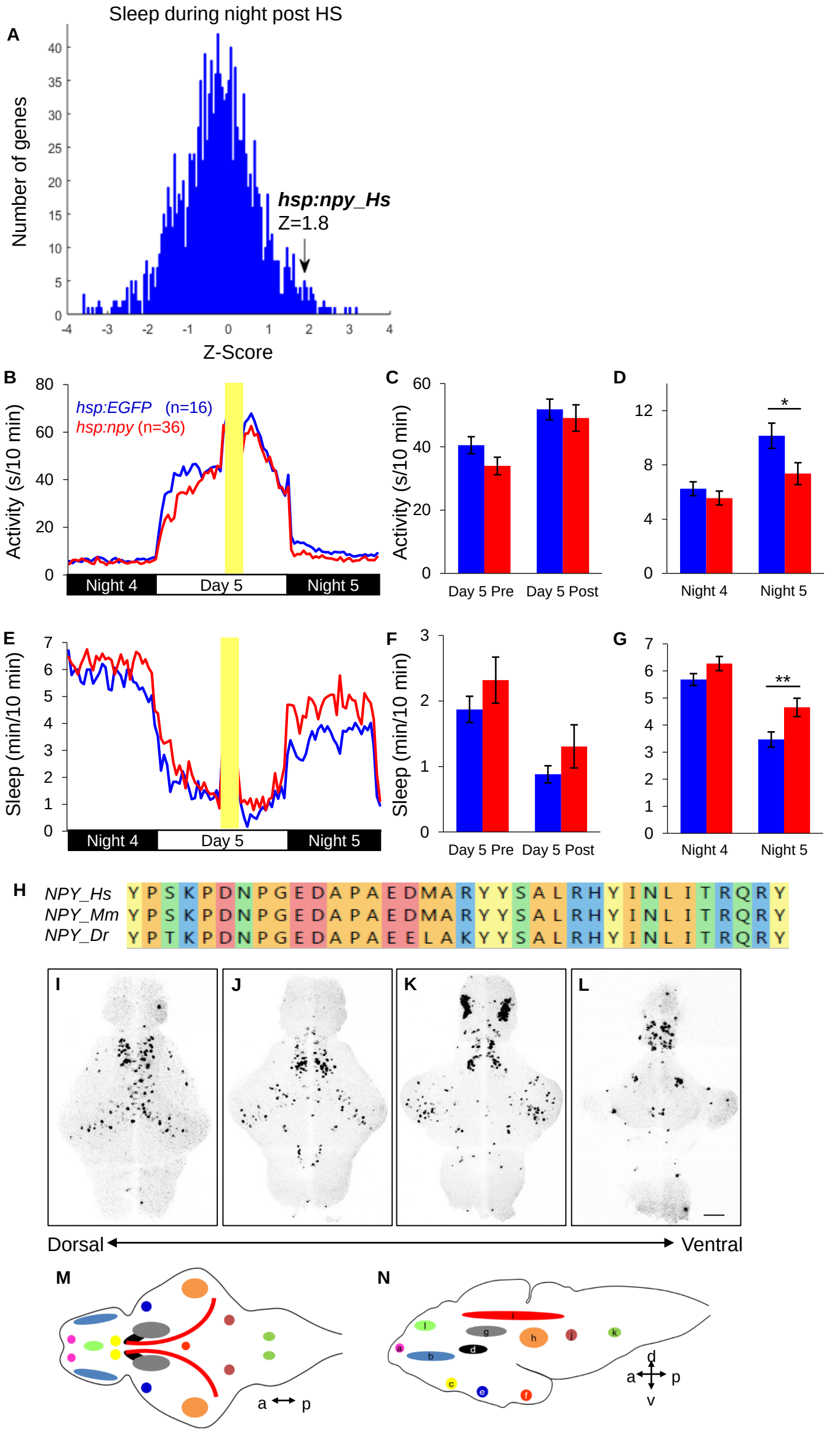

Figure S2. NPY overexpression increases sleep at night and during subjective day in constant dark (Related to Figure 1)

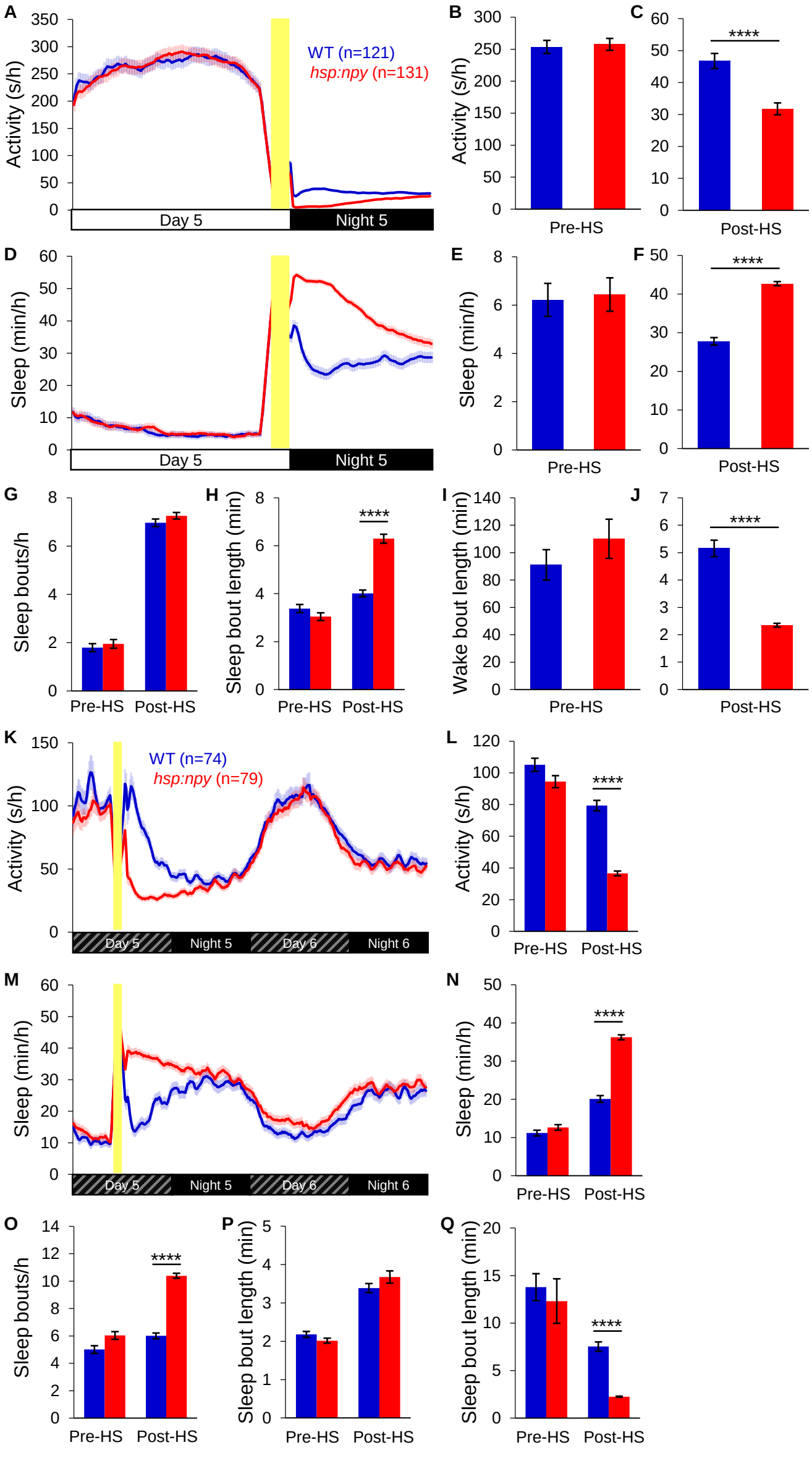

Figure S3. Loss of *npy* reduces daytime sleep before transition to constant light (Related to Figure 3)

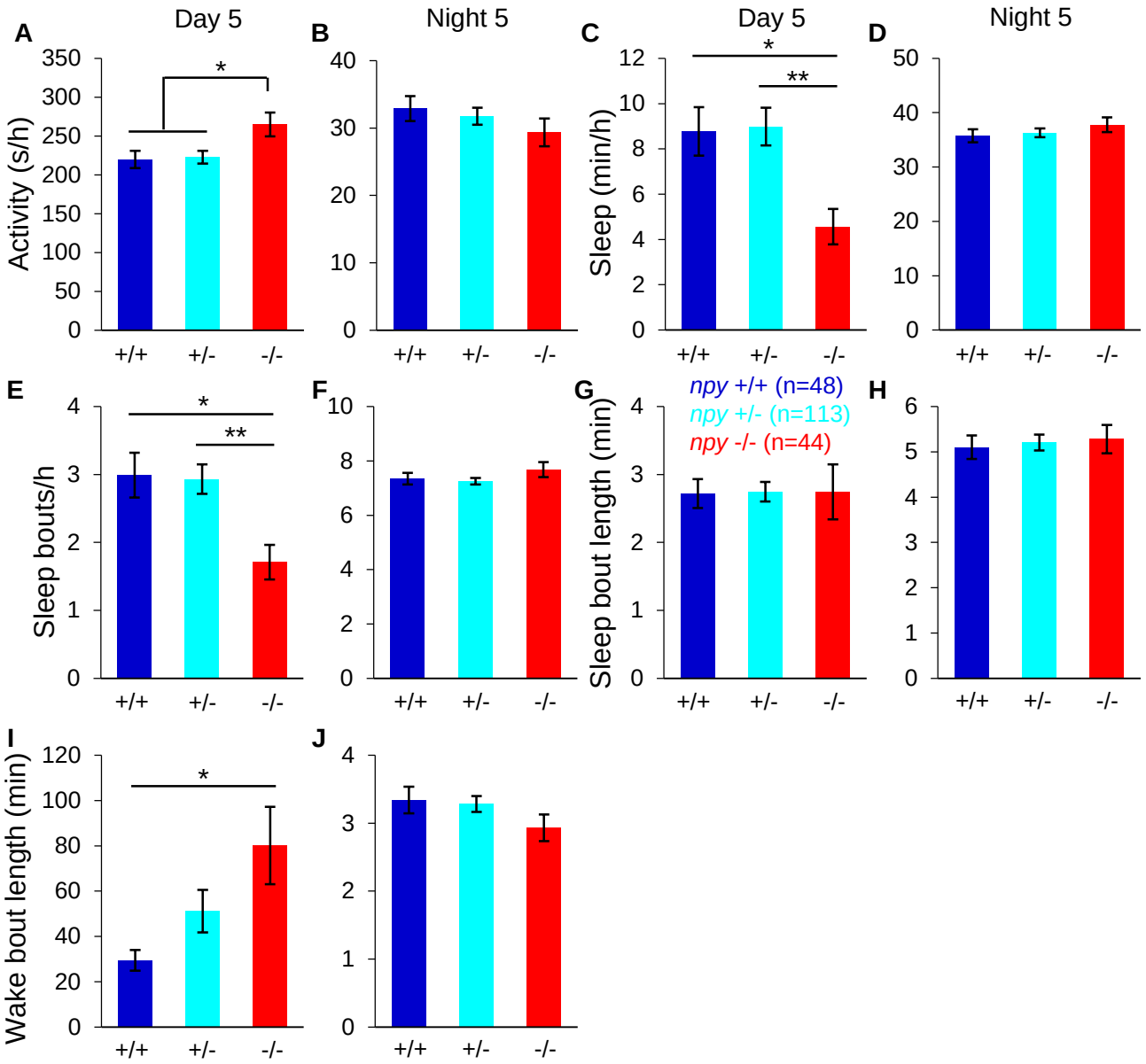

Figure S4. The *npy:kalta4* and *uas:nfsb-mcherry* transgenes do not affect sleep/wake behaviors compared to WT siblings (Related to Figure 4)

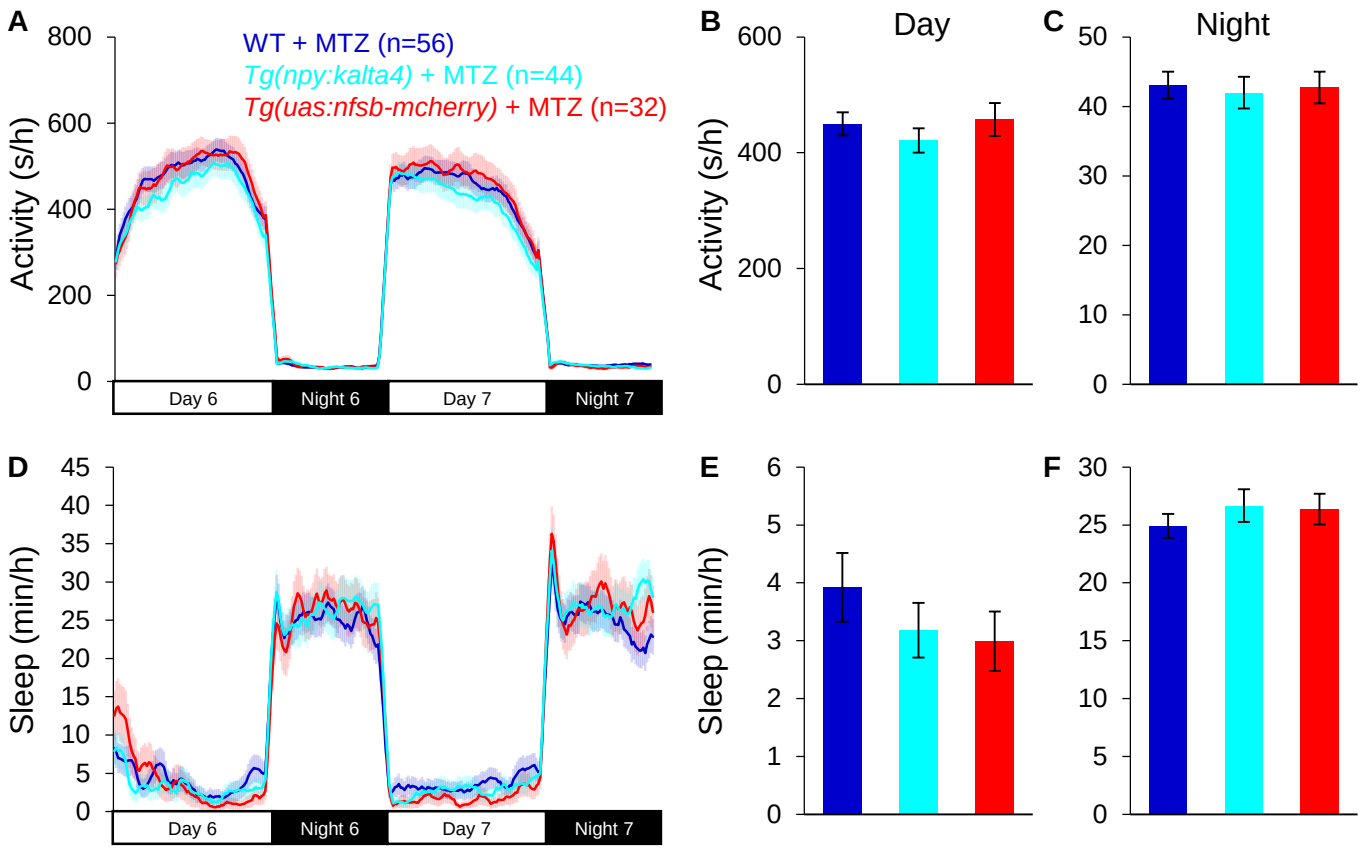

Figure S5. Specific expression of *kalta4* in *npy*-expressing neurons and TUNEL labeling of apoptotic cells (Related to Figure 4)

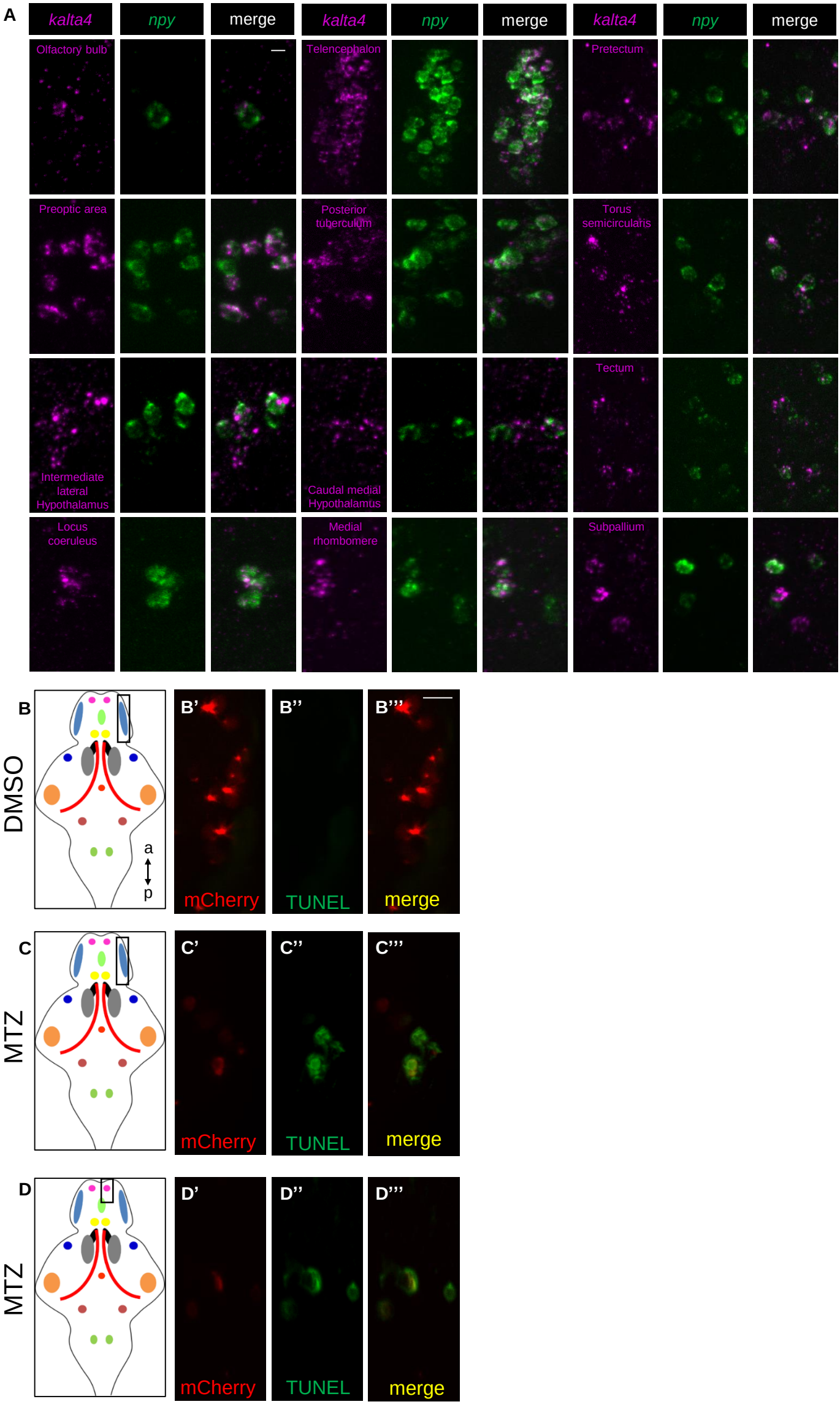

Figure S6. The sedating effects of NPY overexpression and inhibition of NE signaling are not additive (Related to Figure 6)

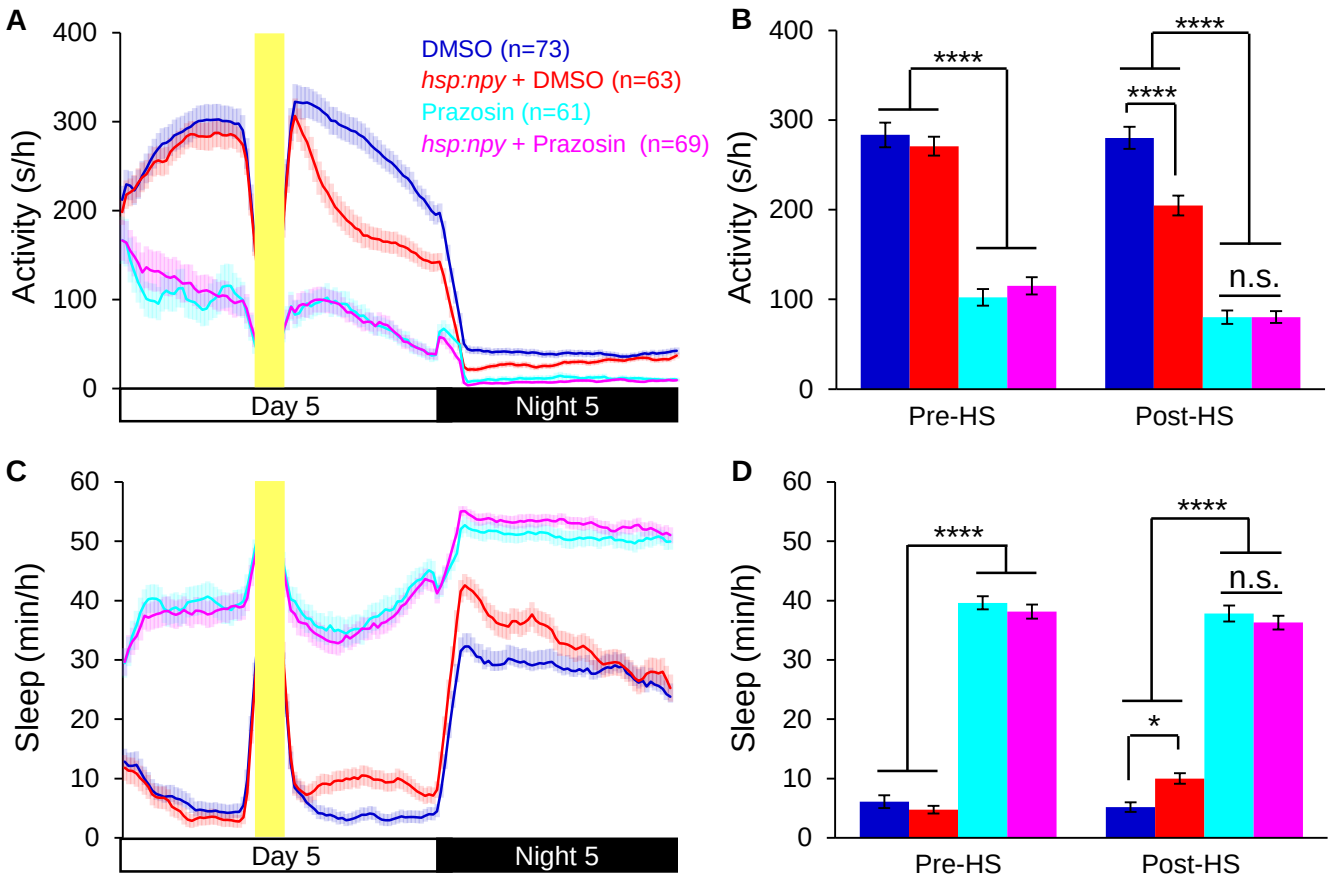

Figure S7. Melatonin enhances sleep induced by overexpression of NPY or by treatment with prazosin (Related to Figure 6)

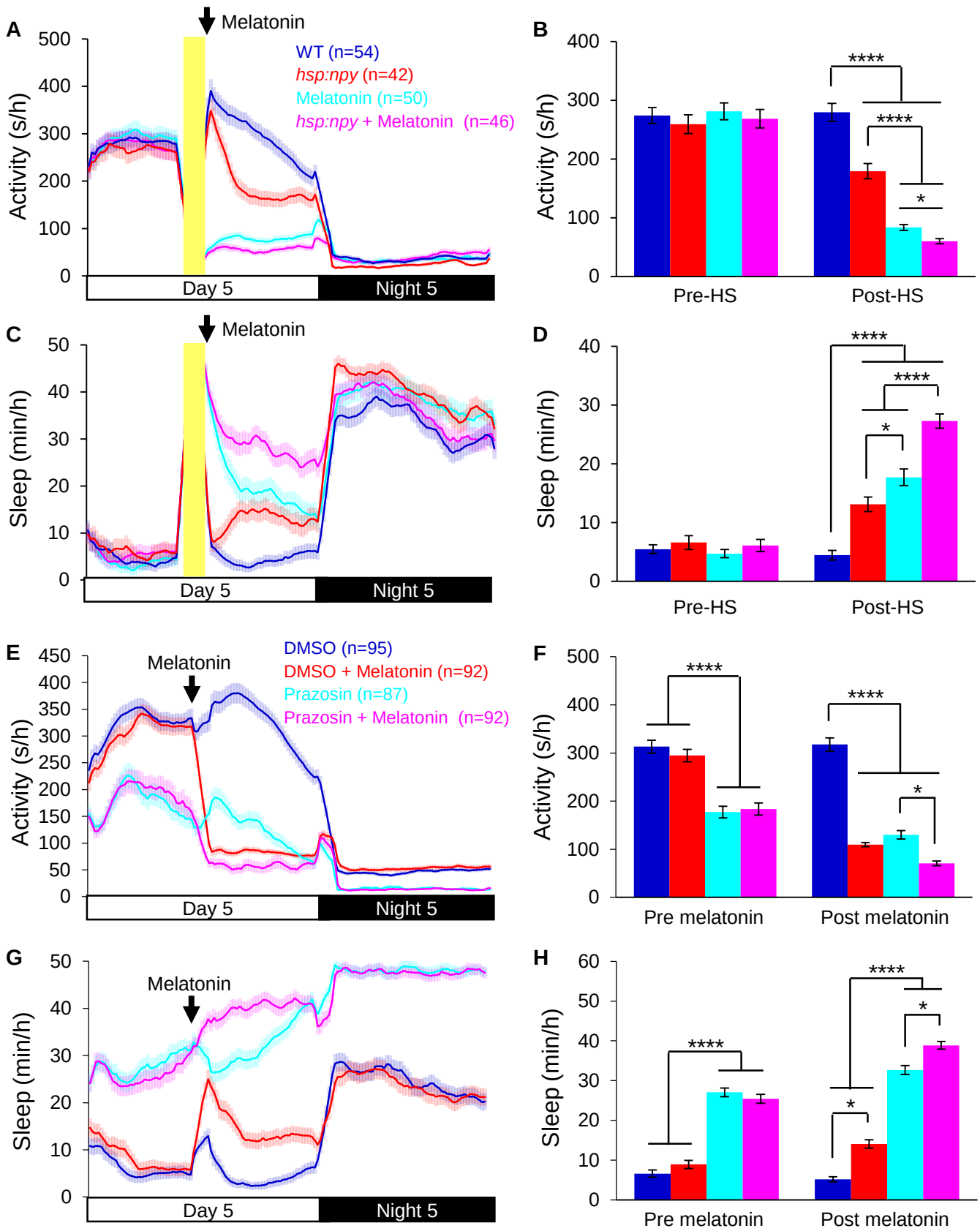

Table S1. Percentage of *npy*-expressing cells that express *kalta4* in *Tg(npy:kalta4)* larvae (Related to Figure 4)

Symbol	Brain region	% *kalta4*-expressing neurons co-expressing *npy*	% *npy* neurons co-expressing *kalta4*
A	Olfactory bulb	100.00 ± 0.00	91.67 ± 6.81
B	Telencephalon	98.92 ± 1.07	95.10 ± 1.97
C	Preoptic area	97.07 ± 1.61	88.71 ± 2.53
D	Posterior tuberculum	98.72 ± 1.28	89.31 ± 3.31
E	Intermediate lateral Hypothalamus	100.00 ± 0.00	94.44 ± 5.56
F	Caudal medial Hypothalamus	100.00 ± 0.00	88.89 ± 11.12
G	Pretectum	98.04 ± 1.96	83.06 ± 1.17
H	Torus semicircularis	95.77 ± 2.41	88.34 ± 4.52
I	Tectum	98.03 ± 0.98	89.09 ± 1.04
J	Locus coeruleus	100.00 ± 0.00	88.89 ± 11.12
K	Medial rhombomere	96.67 ± 3.33	82.22 ± 1.11
L	Subpallium	92.86 ± 5.83	86.61 ± 0.72

Table S2. Mutants and drugs tested for effects on NPY overexpression-induced sleep (Related to Figure 6)

Mutant	System Affected
histidine decarboxylase	no histamine
hypocretin receptor	no hypocretin signaling
corticotropin releasing hormone a	no crha
corticotropin releasing hormone b	no crhb
arylalkylamine N-acetyltransferase 2	no melatonin

Table S3. List of primers used in this study

Genotyping Primers	
Primer Name	**Primer Sequence**
hsp:npy genotype F	CCGCCACCATGAATCCA
hsp:npy genotype R	GGTTTGTCCAAACTCATCAATGT
npy mutant genotype F	ATAAATTGCGCATCAGCACA
npy mutant genotype R	TGAGGAAGAATTTGAGACTACGC
npy:kalta4 genotype F	CGCTATCATTTATAGATTTTTGCAC
npy:kalta4 genotype R	AGTAGCGACACTCCCAGTTG
Primers for Riboprobe Synthesis	
Primer Name	**Primer Sequence**
npy riboprobe F	CCACAGAGCAAGAATTCCAA
npy riboprobe R	CAGTCATTATTGTTCTCCTTTGC
adcyap1a riboprobe F	ATGATTACGAGCAGCAAAACGACTC
adcyap1a riboprobe R	TCACAAAGCCGGGAATTCAG
npyr1 riboprobe F	CTGACCGACAGCAGTGTGTT
npyr1 riboprobe R	CCGGTGGTGTAGGTGAGTTT
npyr2 riboprobe F	CGCAATTTACACACGGTGAC
npyr2 riboprobe R	TCCCTTACTGCCTCACTGCT
npyr2l riboprobe F	GGCTTGTGTGGATGGATGTA
npyr2l riboprobe R	TGTCGAGGTGGTAAACGATG
npyr4 riboprobe F	GTCCTAGGGGTGTGCATGTC
npyr4 riboprobe R	AATAGCAACAAGCTGGTGGTG
npyr7 riboprobe F	AAGAGACCAGCCTGGGAAAT
npyr7 riboprobe R	AAACTGCGAAGACCACGACT
npyr8a riboprobe F	CCAGAAATCATGGGTGGAGT
npyr8a riboprobe R	GCAAATGCAACCACAATCAC
npyr8b riboprobe F	CGAAGCGTTATGCAAAGTGA
npyr8b riboprobe R	TTGCTCAAGATGGAGCCTTT
Primers for BAC transgenesis	
Primer Name	**Primer Sequence**
Homology arm F	AACAATAAATTGCGCATCAGCACAAACACGTTTGCTTTGTTTAATTGCAG
Homology arm R	AAGAGAAACGCGCACGCTGCCCAGCTCATCCACATCTTCATGTTTGGATT
pIndigoBAC_HA1_iTol2_F	TTCTCTGTTTTTGTCCGTGGAATGAACAATGGAAGTCCGAGCTCATCGCTCCCTGCTCGAGCCGGGCCCAAGTG
pIndigoBAC_HA1_iTol2_R	AGCCCCGACACCCGCCAACACCCGCTGACGCGAACCCCTTGCGGCCGCATATTATGATCCTCTAGATCAGATC

SUPPLEMENTAL INFORMATION

SUPPLEMENTAL FIGURE LEGENDS

Figure S1. A genetic screen identifies a sleep-promoting role for NPY and zebrafish *npy* is widely expressed in the brain (Related to Figure 1). (**A**) Histogram depicting the total amount of sleep during the night after heat shock for ~1200 human genes tested in the larval zebrafish genetic screen. Larvae overexpressing human NPY had a Z-score of 1.8. Overexpression of human NPY decreased locomotor activity (**B-D**) and increased sleep (**E-G**) compared to EGFP-overexpressing controls during the night following heat shock (indicated by yellow bar). (**H**) Amino acid sequence alignment of human (Hs), mouse (Mm) and zebrafish (Dr) NPY mature peptide sequences. Colors indicate residues with similar properties. (**I-L**) ISH using an *npy*-specific probe reveals discrete yet widespread nuclei of *npy* expression in a 6-dpf zebrafish. Images show 4 different focal planes, with the most dorsal image at left. The full image stack of *npy* expression throughout the brain mapped onto the Z-brain atlas is shown in **Video S1**. (**M,N**) Schematic drawings illustrate relative positions of different *npy*-expressing populations in ventral (**M**) and lateral (**N**) views. *npy* is expressed in the olfactory bulb (a), telencephalon (b), preoptic area (c), posterior tuberculum (d), Intermediate lateral hypothalamus (e), caudal medial hypothalamus (f), pretectum (g), torus semicircularis (h), tectum (i), locus coeruleus (j), medial rhombomere (k) and subpallium (l)**.** a, anterior; p, posterior; d, dorsal; v, ventral. Scale bar: 100 µm. Mean (**B,E**) and mean ± SEM (**C,D,F,G**) are shown. n=number of animals. **P*<0.05, ***P*<0.01 by two-tailed Student's t test.

Figure S2. NPY overexpression increases sleep at night and during subjective day in constant dark (Related to Figure 1). (**A-J**) Heat shock-induced overexpression of zebrafish NPY during the last hour of the day resulted in decreased locomotor activity (**A-C**) and increased sleep (**D-F**) during the following night. NPY overexpression increased the length of sleep bouts (**H**) and decreased the length of wake bouts (**J**), but did not affect the number of sleep bouts (**G**). Pre-HS

and Post-HS quantify data during the entire day before and entire night after heat shock (indicated by yellow bar in line graphs), respectively. (**K-Q**) Larvae were entrained in 14:10 hour light:dark cycles for 4 days, and then transferred to constant dark after the fourth night of development. Heat shock-induced overexpression of zebrafish NPY during the subjective day resulted in decreased locomotor activity (**K,L**) and increased sleep (**M,N**) during the remainder of the subjective day. NPY overexpression increased the number of sleep bouts (**O**) and decreased the length of wake bouts (**Q**), but had no effect on the length of sleep bouts (**P**). Pre-HS and Post-HS quantify data during the entire subjective day before and after heat shock (indicated by yellow bar in line graphs), respectively. Mean ± SEM from 3 (**A-J**) and 2 (**K-Q**) pooled experiments are shown. n=number of animals. **** $P<0.0001$ by two-tailed Student's t test.

Figure S3. Loss of *npy* reduces daytime sleep in animals raised in LD before transition to LL (Related to Figure 3). Larvae were entrained in 14:10 hour LD cycles for 4 days and then behaviorally monitored for one LD cycle before transferring to LL. During the one LD cycle, *npy*-/- larvae were more active (**A**), and slept less (**C**), than their *npy*+/+ and *npy*+/- siblings during the day. These phenotypes were due to fewer sleep bouts (**E**), and longer wake bouts (**I**). Mean ± SEM from 3 pooled experiments is shown. n=number of animals. *$P<0.05$, **$P<0.01$ by one-way ANOVA with Holm-Sidak post hoc test.

Figure S4. The *npy:kalta4* and *uas:nfsb-mcherry* transgenes do not affect sleep/wake behaviors (Related to Figure 4). *Tg(npy:kalta4)*, *Tg(uas:nfsb-mcherry)* and WT sibling larvae were treated with MTZ from 3-5 dpf, and their behavior was monitored from the morning of 6 dpf until the morning of 8 dpf. Mean ± SEM from 3 pooled experiments is shown. n=number of animals. No significant difference was observed among the three genotypes in their activity (**A-C**) or sleep (**D-F**) ($P>0.05$ by one-way ANOVA with Holm-Sidak post hoc test).

Figure S5. Specific expression of *kalta4* in *npy*-expressing neurons and TUNEL labeling of apoptotic cells (Related to Figure 4). (**A**) Double FISH showing *kalta4* and *npy* co-expression using probes specific for *kalta4* and *npy* in different populations of *npy*-expressing neurons. (**B-D**) *Tg(npy:kalta4)*;*Tg(uas:nfsb-mcherry)* animals were treated with DMSO (**B**) or 10 mM MTZ (**C,D**) from 72-90 hpf, and then fixed and processed for TUNEL. TUNEL labeling was observed in *npy*-expressing neurons of animals treated with MTZ (**C,D**), but not in animals treated with DMSO (**B**). Note that mCherry fluorescence is weaker in MTZ-treated animals because the neurons are undergoing apoptosis. Leftmost panels show schematic brain diagrams with *npy* expression domains colored as in **Figure S1**, and boxes indicate exemplar regions shown in the fluorescent images. a, anterior; p, posterior. Scale bar: 10 µm.

Figure S6. The sedating effects of NPY overexpression and inhibition of NE signaling are not additive (Related to Figure 6). *Tg(hsp:npy)* larvae and their WT siblings were treated with 100 µM prazosin or DMSO vehicle control, and then heat shocked (yellow bar in line graphs) during the fifth day of development. Prazosin-treated animals were less active (**A,B**) and slept more (**C,D**) during the day before and after heat shock. DMSO-treated *Tg(hsp:npy)* animals were less active and slept more than their DMSO-treated WT siblings during the day after heat shock. NPY overexpression did not further decrease locomotor activity or increase sleep in prazosin-treated *Tg(hsp:npy)* animals. Pre-HS and Post-HS quantify data for day 5 before and after heat shock, respectively. Mean ± SEM from 3 pooled experiments is shown. n=number of animals. n.s.=not significant, *P<0.05, ****P<0.0001 by two-way ANOVA with Holm-Sidak post hoc test.

Figure S7. Melatonin treatment enhances sleep induced by overexpression of NPY or by treatment with prazosin (Related to Figure 6). (**A-D**) *Tg(hsp:npy)* animals and their WT siblings were heat shocked (yellow bar in line graphs) during the fifth day of development, after which 20 µM melatonin was added (arrow in line graphs). *Tg(hsp:npy)* animals were less active (**A,B**) and

slept more (**C,D**) than their WT siblings after heat shock. Both *Tg(hsp:npy)* and their WT siblings showed a further decrease in activity (**A,B**) and increase in sleep (**C,D**) after addition of melatonin. Pre-HS and Post-HS quantify data for day 5 before and after heat shock, respectively. (**E-H**) WT animals were treated with either 100 µM prazosin or DMSO vehicle control starting at 4 dpf, and 20 µM melatonin was added during the fifth day of development (arrow in line graphs). Prazosin-treated animals were less active (**E,F**) and slept more (**G,H**) than DMSO-treated siblings. Both prazosin- and DMSO-treated animals showed a further decrease in activity (**E,F**) and increase in sleep (**G,H**) following addition of melatonin. Pre melatonin and Post melatonin quantify data for day 5 before and after addition of melatonin, respectively. Mean ± SEM for 2 (**A-D**) and 3 (**E-H**) pooled experiments are shown. n=number of animals. **P*<0.05, *****P*<0.0001 by two-way ANOVA with Holm-Sidak post hoc test.

Table S1. Percentage of *npy*-expressing cells that express *kalta4* in *Tg(npy:kalta4)* larvae (Related to Figure 4). The specificity of *kalta4* expression in *Tg(npy:kalta4)* animals at 5 dpf was assayed by double FISH using probes specific for *kalta4* and *npy* and quantified in each sub-population of *npy*-expressing neurons. Mean ± SEM percentage of co-expression in 4 animals is shown.

Table S2. Mutants tested for effects on NPY overexpression-induced sleep (Related to Figure 6). The effect of NPY overexpression on locomotor activity and sleep was compared in animals that were homozygous mutant for each of the indicated genes to their WT siblings. In each case an additive phenotype was observed.

Table S3. List of primers used in this study.

Video S1. Annotation of *npy* expression domains in the zebrafish brain (Related to Figure 1). *In situ* hybridization with an *npy*-specific probe was performed on 6 dpf larval zebrafish brains, followed by immunostaining for t-ERK. The t-ERK staining was then used to register *npy* expression to the Z-brain reference brain. Anatomical domains of *npy* expression were then added using the Z-Brain browser annotations. Anterior is to the left and the video starts from the ventral surface of the brain. The video does not show the expression of *npy* expression in the olfactory bulb or retina.

Video S2. Hindbrain *npy*-expressing neurons project to the LC (Related to Figure 5). Projections from hindbrain *npy*-expressing neurons (blue) and *dbh*-expressing LC neurons (yellow) form close contacts. An exemplar *npy*-expressing neuron (hightlighted magenta) appears to contact a single *dbh*-expressing neuron (highlighted green) at least twice (white, indicated by asterisk, magnified 4-fold in insets). Scale bar: 10 µm.

Supplemental Movie 1

Click here to access/download

Supplemental Movies and Spreadsheets

Video S1.mp4

Supplemental Movie 2

Click here to access/download

Supplemental Movies and Spreadsheets

Video S2.avi